

# Integrated Colours of Milky Way Globular Clusters and Horizontal Branch Morphology

G. H. SMITH<sup>1</sup> and J. STRADER<sup>1</sup>

University of California Observatories/Lick Observatory, Department of Astronomy and Astrophysics, University of California, Santa Cruz, 95064 USA

Received; accepted; published online

**Abstract.** Broadband colours are often used as metallicity proxies in the study of extragalactic globular clusters. A common concern is the effect of variations in horizontal branch (HB) morphology — the second-parameter effect — on such colours. We have used *UBVI*, Washington, and DDO photometry for a compilation of over 80 Milky Way globular clusters to address this question. Our method is to fit linear relations between colour and [Fe/H], and study the correlations between the residuals about these fits and two quantitative measures of HB morphology. While there is a significant HB effect seen in  $U - B$ , for the commonly used colours  $B - V$ ,  $V - I$ , and  $C - T_1$ , the deviations from the baseline colour-[Fe/H] relations are less strongly related to HB morphology. There may be weak signatures in  $B - V$  and  $C - T_1$ , but these are at the limit of observational uncertainties. The results may favour the use of  $B - I$  in studies of extragalactic globular clusters, especially when its high [Fe/H]-sensitivity is considered.

**Key words:** galaxies: star clusters – globular clusters: general – stars: horizontal-branch

©0000 WILEY-VCH Verlag GmbH & Co. KGaA, Weinheim

## 1. Introduction

Integrated photometry has become a widely-used tool for the investigation of globular cluster (GC) systems in galaxies, dating back to the work of van den Bergh (1967), who demonstrated that a reddening-independent index formed from the *UBV* colours of Milky Way GCs could be correlated with metallicity. Despite several associated problems, it seems likely that integrated colours will continue to be used as metallicity proxies for extragalactic globular cluster systems that are beyond the reach of spectroscopic study. It also seems likely that the globular clusters of the Milky Way will continue to be used as calibrators for such studies. Calibrations have been published in a number of photometric systems (e.g., Aaronson et al. 1978; Frogel, Persson, & Cohen 1980; Bica & Pastoriza 1983; Brodie & Huchra 1990; Geisler & Forte 1990; Cohen & Matthews 1994). For the purposes of studying globular clusters in M31, Barmby et al. (2000) derived observational colour-metallicity relations for Milky Way GCs in a variety of broadband colours; these relations are in wide use.

There have also been a number of efforts to reproduce the integrated colours of Milky Way globular clusters with stel-

lar population models, since these clusters form one of the best “control” samples for such tests. For example, Barmby & Huchra (2000) compared the integrated colours of globular clusters in the Milky Way and M31 with population synthesis models of Bruzual & Charlot (as reported in Leitherer et al. 1996), and Kurth, Fritz-von Alvensleben, & Fricke (1999), as well as updated versions of the Worthey (1994) models. They concluded that an age difference of 4 Gyr or more was needed between metal-rich and metal-poor clusters in order to provide the best model fits to their colours, with the metal-rich clusters being systematically younger. Covino et al. (1994) used theoretical stellar spectral energy distributions to model the integrated colours of star clusters, and to explore their sensitivity to metallicity, horizontal branch (HB) morphology, red giant mass loss, and stellar mass function. They concluded that integrated colours are more sensitive to the first two of these factors. Maraston (1998) used evolutionary population synthesis models to calculate the changes in integrated *UBV* colours caused by adding blue horizontal branch stars to a 15 Gyr solar abundance model population. She found both  $B - V$  and  $U - B$  to be altered by  $\sim 0.10$  to  $0.15$  mag by the addition of a blue horizontal branch (BHB) population. Further modelling was done by Brocato et al. (2000), who explored the sensitivity of integrated colours to both age

and statistical fluctuations in the number of bright giants. The Brocato et al. (2000) models show that, particularly at low metallicity, the integrated  $U - B$ ,  $B - V$  and  $V - I$  colours are sensitive to the value of the Reimers mass-loss parameter  $\eta$  for red giants, since this affects the masses and temperatures of stars on the horizontal branch. A detailed discussion is given by Yi (2003).

Other theoretical studies have demonstrated that in addition to metallicity and age, the integrated spectra and hydrogen line strengths of globular clusters should be sensitive to the temperature distribution of horizontal branch stars, particularly those hotter than the RR Lyrae variables (Lee, Yoon, & Lee 2000; Maraston & Thomas 2000). On the observational side, de Freitas Pacheco & Barbuy (1995) showed that the strength of the  $H\beta$  line in the integrated spectra of Milky Way GCs was a “bivariate function of metallicity and a parameter describing the horizontal branch morphology.” They found that BHB stars can make “a substantial contribution” to the  $H\beta$  line-strength. This influence of HB stars has been a concern in the interpretation of integrated spectra of globular clusters, in part because of the difficulty of disentangling their effects from those of age differences (e.g., Peterson et al. 2003; Schiavon et al. 2004). Modeling performed by Puzia et al. (2005) and Maraston (2005) suggests that BHB stars in metal-rich clusters can increase the value of the Lick  $H\beta$  index by 0.4 Å or greater, reducing derived ages by 5 Gyr or more. Colours based on filter bandpasses containing significant Balmer line absorption might therefore be sensitive to horizontal branch morphology.

The main question addressed in this paper is whether a dependence upon horizontal branch morphology can be discerned in the integrated-light colours of Milky Way globular clusters. Our approach is to investigate whether the scatter in various integrated colour-metallicity relations is correlated with parameters describing the horizontal branch structure. In addition, we check for correlations with several other cluster properties, such as central concentration and stellar mass function. Much of the focus of this paper is on colour systems that include filters with passbands in the violet or ultraviolet regions of the spectrum, where blue horizontal branch stars are most likely to have an influence on integrated cluster magnitudes. The colours that we investigate are those of the Johnson  $UBV$ , the Cousins  $VI$ , the DDO, and Washington systems.

## 2. *UBVI Colours*

### 2.1. *The Colour and Metallicity Data Base*

We have collected both  $UBVI$  and DDO colours for the combined set of Milky Way globular clusters observed by McClure & van den Bergh (1968; MV68) and Bica & Pastoriza (1983; BP83). The primary source consulted for dereddened  $(U - B)_0$ ,  $(B - V)_0$ ,  $(V - I)_0$  colours and associated reddenings is Reed, Hesser, & Shawl (1988; RHS88). They employed a database of observed colours having been compiled by Reed (1985), who homogenised data from 18 different literature sources. The majority of the data consist of aper-

ture photometry obtained with 1P21 photomultipliers, with several sources (Hamuy 1984, Hanes & Brodie 1985) having used S20 photomultipliers in order to obtain  $I$ -band data. The resulting colours are on the  $UBV$  system defined by the measurements of van den Bergh (1967) and the  $VRI$  system defined by the measurements of Hamuy (1984). As shown by Racine (1973), the reddening ratio  $E(U - B)/E(B - V)$  of globular clusters varies with the spectral type of the integrated light, increasing in value towards later spectral type. The primary objectives of Reed et al. (1988) were to determine the relationships between various integrated colours as a function of cluster spectral type, and to thereby obtain values of various interstellar-reddening ratios as a function of spectral type. Reddenings and intrinsic colours were derived for each cluster in their sample, and we have adopted their values for the intrinsic colours.

Reed et al. (1988) did not present any detailed discussion of the uncertainties in the  $UBVI$  colours. Reed (1985) gives values of a quantity denoted  $\langle \text{RESIDUALS} \rangle$  that reflects the scatter among the colour measurements of each cluster from his various sources. It is equivalent to  $\langle |C_i - \langle C_i \rangle| \rangle$ , where the brackets refer to weighted averages, and  $C_i$  to the colour measurement for a given cluster from source  $i$  after transformation onto a uniform scale. Hamuy (1984) has compared his  $U - B$ ,  $B - V$ ,  $V - R$ , and  $R - I$  measurements with the colours from Harris & Racine (1979), who in turn list averages from different sources, and the observations of Hanes & Brodie (1985). He finds that systematic differences between these sources can range from 0.01 to 0.03 mag, with scatters of  $\pm 0.04$  mag for the  $UBV$  colours and  $\pm 0.05$  mag for  $VRI$ .

Where available, metallicities were compiled from the homogeneous data set of Rutledge et al. (1997a,b). They are based on the combined strengths of the  $\lambda 8498$ ,  $\lambda 8542$ , and  $\lambda 8662$  Ca II triplet lines of red giant branch (RGB) stars that are probable GC members. Rutledge et al. (1997a,b) followed the techniques of Armandroff & Da Costa (1991) for measuring the equivalent widths of these lines, correcting them to a reference point on the RGB equal to the  $V$  magnitude of the horizontal branch, and correlating them against various  $[\text{Fe}/\text{H}]$  measurements. The metallicities given in column 5 of Table 2 of Rutledge et al. (1997b) were adopted in this study, this column containing their “most probable”  $[\text{Fe}/\text{H}]$  value on the scale of Zinn & West (1984; ZW84). Since the Rutledge et al. (1997b) metallicities are based on spectroscopy of individual cluster red giants (typically  $\sim 10$ -20 per cluster, Rutledge et al. 1997a), they should not be subject to horizontal branch effects in the way that metallicity estimates based on integrated cluster-light techniques could be. Where not available from this source, values of  $[\text{Fe}/\text{H}]$  for the clusters in our compilation were adopted from Table 6 of ZW84.

Reddenings for the clusters included in this study are available from both Reed et al. (1988) and the 1999 version (designated elsewhere in this paper as H99) of the catalogue of Milky Way GC properties described by Harris (1996). We have tended to use the more recent reddenings from H99 for the purposes of dividing our cluster sample up into different reddening groups.

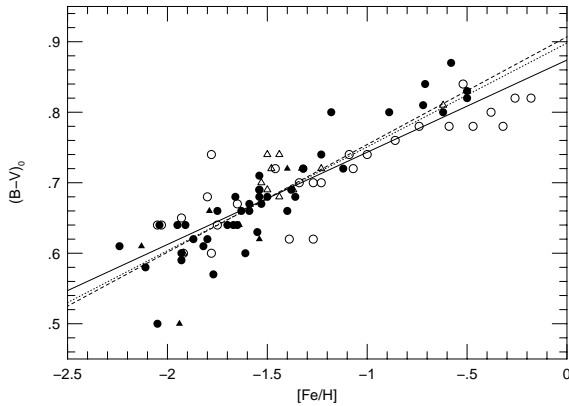


**Fig. 1.** The integrated  $(B - V)_0$  colour of Milky Way globular clusters plotted versus metallicity  $[\text{Fe}/\text{H}]$ . Triangles represent core-collapse clusters, filled and open symbols correspond to clusters with reddenings of  $E(B - V)_{\text{H99}} \leq 0.3$  and  $E(B - V)_{\text{H99}} > 0.3$  respectively. Three different linear least-squares fits are shown: a fit made to all clusters in the sample (solid line); only clusters with  $E(B - V)_{\text{H99}} \leq 0.5$  (dotted line); and only those clusters with both  $E(B - V)_{\text{H99}} \leq 0.5$  and  $[\text{Fe}/\text{H}] < -0.5$  (dashed line).

## 2.2. UBVI Colour-Metallicity Relations

Plots of  $(B - V)_0$ ,  $(U - B)_0$ , and  $(V - I)_0$  against  $[\text{Fe}/\text{H}]$  are shown in Figures 1 through 3. Symbols used in these figures denote both reddening as taken from H99 (filled symbols for  $E(B - V) \leq 0.3$ , open symbols for greater reddening), and whether a cluster has a core-collapse structure (triangle) or not (circle). Linear regression fits of each colour  $C$  versus  $[\text{Fe}/\text{H}]$  were computed using  $\chi^2$  minimisation. Fits were made by minimising unweighted colours. Values of the coefficients for a variety of fits of the form  $C = \alpha + \beta[\text{Fe}/\text{H}]$  are given in Table 1, together with the variances  $\sigma(\alpha)$  and  $\sigma(\beta)$ , and a measure of the standard deviation in the GC colour residuals about each fit,

$$\sigma_C = \sqrt{\frac{\sum_{n=1}^N (C_n - \alpha - \beta[\text{Fe}/\text{H}]_n)^2}{N - 2}}, \quad (1)$$

where  $N$  is the number of clusters fitted, and  $C_n$  and  $[\text{Fe}/\text{H}]_n$  are the colour and metallicity of the  $n$ th cluster (Press et al. 1999). Each colour-metallicity fit is labelled with a letter in the first column of Table 1, and the eighth column specifies the clusters used in computing that fit.

In plots of  $(B - V)_0$  and  $(U - B)_0$  versus  $[\text{Fe}/\text{H}]$  there seems to be some separation between clusters with  $E(B - V) \leq 0.3$  and  $E(B - V) > 0.5$  at metallicities of  $[\text{Fe}/\text{H}] > -0.5$ . Consequently, for these colours, fits were computed for several different samples: (i) no constraint on either  $E(B - V)$  or  $[\text{Fe}/\text{H}]$ , (ii) only clusters with reddenings from H99 of  $E(B - V)_{\text{H99}} < 0.5$ , and (iii) only clusters with reddenings of  $E(B - V)_{\text{H99}} < 0.5$  and metallicity  $[\text{Fe}/\text{H}] < -0.5$ . Subsets (ii) and (iii) differ only in the object NGC 5927, which is excluded from sample (iii) on account of

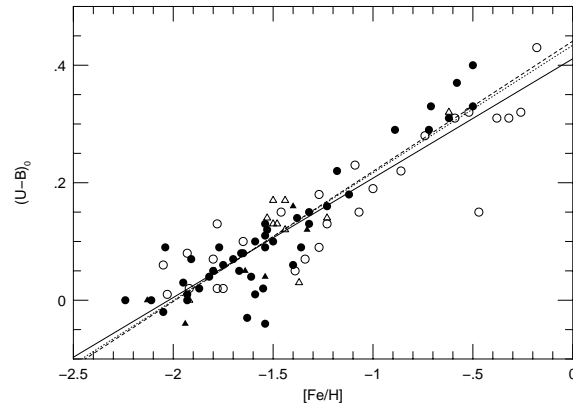


**Fig. 2.** The integrated  $(U - B)_0$  colour of Milky Way globular clusters plotted versus metallicity  $[\text{Fe}/\text{H}]$ . Triangles represent core-collapse clusters, filled and open symbols correspond to clusters with reddenings of  $E(B - V)_{\text{H99}} \leq 0.3$  and  $E(B - V)_{\text{H99}} > 0.3$  respectively. Three different linear least-squares fits are shown: a fit made to all clusters in the sample with the exception of NGC 6316 (solid line); only clusters with  $E(B - V)_{\text{H99}} \leq 0.5$  (dotted line); and only those clusters with both  $E(B - V)_{\text{H99}} \leq 0.5$  and  $[\text{Fe}/\text{H}] < -0.5$  (dashed line).

a high metallicity. The cluster NGC 6316 has been excluded from all fits involving  $(U - B)_0$  due to a discordant position in Figure 2. Fits based on subset (iii) will be less subject to any non-linearity that may exist at high  $[\text{Fe}/\text{H}]$  in the colour-metallicity relations.

The bottom panel of Figure 3 shows all clusters with  $(V - I)_0$  measurements, while in the top panel only clusters with  $E(B - V)_{\text{H99}} \leq 0.3$  are shown. The scatter in  $(V - I)_0$  at a given  $[\text{Fe}/\text{H}]$  is larger than for either  $(U - B)_0$  or  $(B - V)_0$ . It is possible that this reflects larger observational uncertainties in  $V - I$ . Some evidence for this comes from the entries in the  $\langle \text{RESIDUALS} \rangle$  column of Table III of Reed (1985). These residuals are stated to give “an idea of the uncertainties attendant to the final results.” They are often higher for  $V - I$  than for either  $U - B$  or  $B - V$ , being 0.06–0.10 mag for some clusters, consistent with  $V - I$  being the most uncertain of the colours in Reed’s homogenised data set. However, in comparing his  $V - R$  and  $R - I$  photometry with that of Hanes & Brodie (1985), Hamuy (1984) found a scatter of  $\pm 0.05$  mag, which is only slightly larger than the scatter between his  $UBV$  colours and those compiled by Harris & Racine (1979). Three linear fits were made to the  $(V - I)_0$  versus  $[\text{Fe}/\text{H}]$  relation: (i) all clusters regardless of reddening, (ii) clusters with reddenings of  $E(B - V)_{\text{H99}} \leq 0.5$ , and (iii) clusters with  $E(B - V)_{\text{H99}} \leq 0.3$ .

With regards to the  $(U - B)_0$  and  $(B - V)_0$  colours, the fits for the more restricted samples with lower reddenings have slightly greater slopes,<sup>1</sup> but the rms scatter about the fits

<sup>1</sup> This may provide some evidence that the colour- $[\text{Fe}/\text{H}]$  relations are slightly flatter at high metallicities, i.e., that they are non-

**Table 1.** Coefficients in colour-metallicity relations: Colour =  $\alpha + \beta[\text{Fe}/\text{H}]$ 

Fit	Colour	$\alpha$	$\sigma(\alpha)$	$\beta$	$\sigma(\beta)$	$\sigma_C^1$	Sample
A	$(U - B)_0$	0.411	0.014	0.2032	0.0095	0.046	all clusters from MV68 and BP83 except NGC 6316
B	$(U - B)_0$	0.434	0.017	0.2171	0.0111	0.044	$E(B - V)_{\text{H99}} \leq 0.5$ (which also excludes NGC 6316)
C	$(U - B)_0$	0.441	0.018	0.2215	0.0115	0.044	$E(B - V)_{\text{H99}} \leq 0.5$ and $[\text{Fe}/\text{H}] \leq -0.5$
D	$(B - V)_0$	0.874	0.011	0.1307	0.0078	0.039	all clusters from MV68 and BP83
E	$(B - V)_0$	0.898	0.014	0.1474	0.0094	0.037	$E(B - V)_{\text{H99}} \leq 0.5$
F	$(B - V)_0$	0.907	0.015	0.1530	0.0095	0.036	$E(B - V)_{\text{H99}} \leq 0.5$ and $[\text{Fe}/\text{H}] \leq -0.5$
G	$(V - I)_0$	1.097	0.023	0.1089	0.0157	0.076	all clusters from MV68 and BP83
H	$(V - I)_0$	1.124	0.023	0.1324	0.0148	0.056	$E(B - V)_{\text{H99}} \leq 0.5$
I	$(V - I)_0$	1.164	0.025	0.1583	0.0162	0.049	$E(B - V)_{\text{H99}} \leq 0.3$
J	$(B - I)_0$	2.373	0.038	0.4393	0.0261	0.126	all clusters from MV68 and BP83
K	$(B - I)_0$	2.501	0.037	0.5268	0.0245	0.092	$E(B - V)_{\text{H99}} \leq 0.5$ and $[\text{Fe}/\text{H}] \leq -0.5$
a	$C_0(42 - 45)$	0.808	0.010	0.1553	0.0066	0.033	excludes NGC 6144, 6325, 6517
b	$C_0(38 - 42)$	0.893	0.017	0.2291	0.0111	0.041	excludes NGC 6553
c	$C_0(35 - 38)$	-0.428	0.017	-0.0803	0.0110	0.039	all clusters from MV68 and BP83
d	$C_0(35 - 38)$	-0.439	0.019	-0.0897	0.0120	0.032	$E(B - V)_{\text{H99}} \leq 0.3$
e	$C_0(35 - 42)$	0.468	0.023	0.1508	0.0148	0.051	all clusters from MV68 and BP83
f	$(C - T_1)_0$	1.727	0.029	0.3475	0.0194	0.076	all clusters from H&C77
g	$(C - M)_0$	0.984	0.019	0.2654	0.0127	0.050	all clusters from H&C77
h	$(M - T_1)_0$	0.743	0.011	0.0820	0.0075	0.029	all clusters from H&C77

<sup>1</sup> A measure of the standard deviation of cluster colour about the fitted colour-metallicity relation. The subscript  $C$  refers to the colour that is listed in the second column of each row.

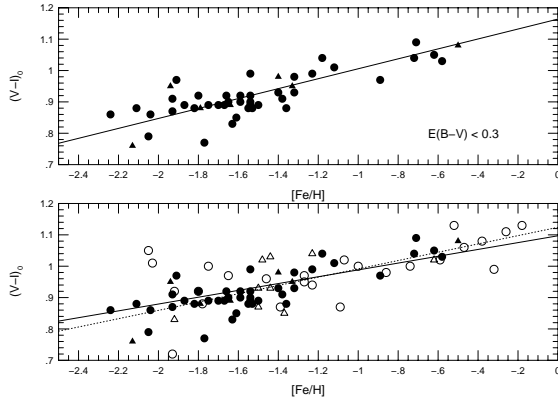


**Fig. 3.** The integrated  $(V - I)_0$  colour of Milky Way globular clusters versus  $[\text{Fe}/\text{H}]$  metallicity. Symbols are the same as for Figures 1 and 2. The bottom panel shows the full cluster sample, while in the top panel only clusters with reddening  $E(B - V)_{\text{H99}} \leq 0.3$  are plotted. Linear least-squares regressions of  $(V - I)_0$  versus  $[\text{Fe}/\text{H}]$  are shown for three different cluster sets: all clusters regardless of reddening (solid line in lower panel), clusters with reddening  $E(B - V)_{\text{H99}} \leq 0.5$  (dotted line in lower panel), and clusters with  $E(B - V)_{\text{H99}} \leq 0.3$  (solid line in top panel).

is little different between the various cases. In all three fits involving the  $(V - I)_0$  colour the rms scatter is larger than for either the  $(U - B)_0$  or  $(B - V)_0$  fits. The values of  $\beta$  linear. However, since many of the high-metallicity GCs are also highly reddened, it is not clear to what extent the differences in slope could be due to uncertainties in their intrinsic colours.

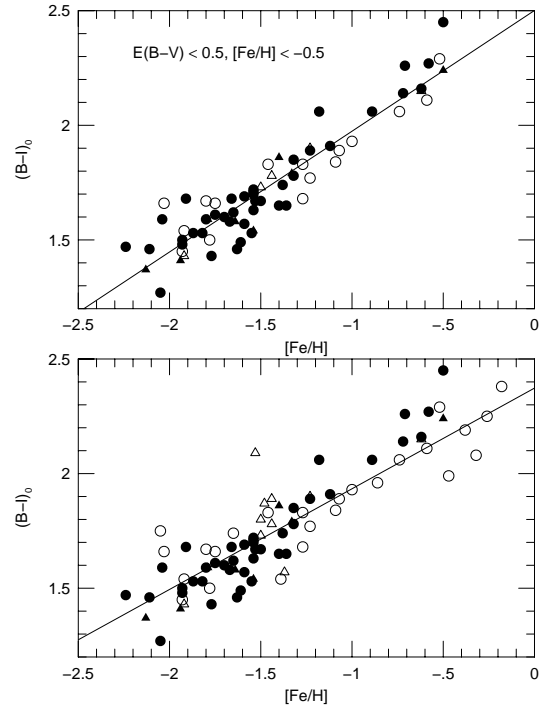


**Fig. 4.** The integrated  $(B - I)_0$  colour of Milky Way globular clusters versus  $[\text{Fe}/\text{H}]$  metallicity. Symbols are the same as for Figures 1 and 2. The bottom panel shows the full cluster sample, while in the top panel only clusters with reddening  $E(B - V)_{\text{H99}} \leq 0.5$  and  $[\text{Fe}/\text{H}] \leq -0.5$  are plotted. Linear least-squares regressions of  $(B - I)_0$  versus  $[\text{Fe}/\text{H}]$  are shown for each sample.

for the various fits indicate that  $V - I$  and  $B - V$  are similar in metallicity sensitivity. By comparison, the  $(U - B)_0$  fits have both less scatter and greater metallicity sensitivity. If the greater scatter in the  $(V - I)_0$ -[Fe/H] relation is intrinsic to the clusters, rather than being due to observational errors, then the utility of this colour as a metallicity indicator would be somewhat compromised.

The behaviour of  $(B - I)_0$ , calculated from the  $(B - V)_0$  and  $(V - I)_0$  values of Reed et al. (1988), is shown as a function of [Fe/H] in Figure 4. Symbols again denote reddening and core structure as in previous diagrams. In the lower panel all clusters are plotted irrespective of reddening or metallicity; in the upper panel only GCs with  $E(B - V)_{\text{H99}} \leq 0.5$  and  $[\text{Fe}/\text{H}] \leq -0.5$  are presented. Linear least-squares fits are shown to both samples, and the derived coefficients are listed in Table 1.

### 2.3. Residuals About the UBVI Colour-Metallicity Relations

Colour residuals were measured with respect to the fits summarised in Table 1. Throughout Section 2 we use the notation  $\delta C_X$  to refer to residuals that have been measured in a colour  $C$  relative to fit X from Table 1. Values of the Pearson linear correlation coefficient<sup>2</sup>  $r$  (Press et al. 1999) between these colour residuals and a variety of GC parameters are listed in Table 2. These results are discussed in Sections 2.5 and 2.6. First, it is necessary to investigate whether the residuals may be affected by imperfectly known cluster reddenings.

The values of  $\delta(V - I)_G$  and  $\delta(U - B)_A$  are plotted versus  $\delta(B - V)_D$  in Figure 5. The residuals shown are those measured with respect to the least-squares fits labelled A, D and G in Table 1, i.e., those fits made to the full sample of clusters unrestricted with respect to reddening or metallicity. The solid lines shown in Figure 5 pass through the origin and have slopes corresponding to reddening vectors of  $E(U - B)/E(B - V) = 0.69$  and  $0.96$  (lower panel), and  $E(V - I)/E(B - V) = 1.14$  and  $1.35$  (upper panel). These reddening ratios correspond to the limits found by Reed et al. (1988) for the earliest and latest spectral-type clusters. If the observed scatter about the various colour-metallicity fits were due entirely to reddening errors, then clusters should fall between the solid lines in Figure 5. Given the addition of measurement errors of  $\approx 0.04$ - $0.05$  mag in the colours, there do seem to be trends in Figure 5 that could be partly accounted for by errors in cluster reddenings. We performed Spearman rank correlation tests (Spearman 1904) among the colour residuals. In the case of  $\delta(U - B)_A$  versus  $\delta(B - V)_D$ , the resulting two-tailed  $p$ -value is  $2 \times 10^{-9}$ , while for  $\delta(V - I)_G$  versus  $\delta(B - V)_D$  we get  $p = 2 \times 10^{-5}$ . In general,  $p$ -values less than about 0.01 to 0.05 are considered to be significant. The value of the Pearson  $r$  parameter is 0.556 and 0.184 respectively. Thus, there does appear to be a correlation between  $\delta(U - B)_A$  and  $\delta(B - V)_D$  that could be consistent, at least for some clusters, with errors in

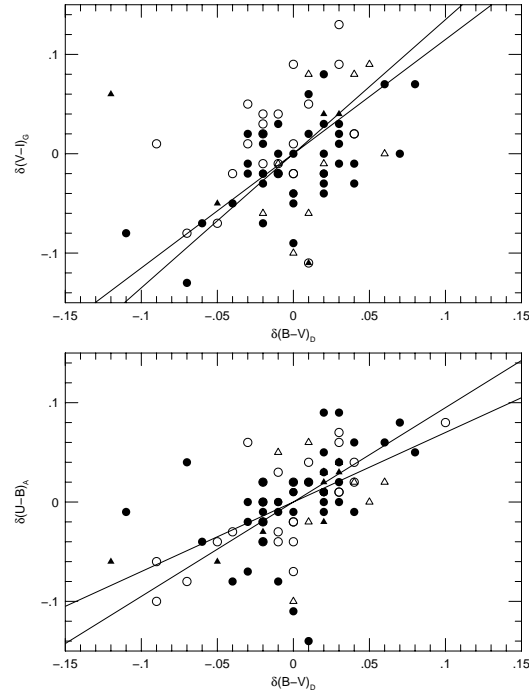


**Fig. 5.** Relationships between residuals about three different colour-metallicity relations for Milky Way globular clusters. The linear least-squares fits about which these residuals were determined are based on the full sample of clusters from MV68 and BP83 unrestricted in metallicity or reddening. The coefficients of these fits are given in the rows labelled A, D, and G in Table 1. The solid lines in each panel have slopes equal to the minimum and maximum values of the reddening ratios  $E(U - B)/E(B - V)$  and  $E(V - I)/E(B - V)$  found by Reed et al. (1988; RHS88) for Milky Way globular clusters. Symbols are the same as for Figure 1 and 2.

reddening. The situation for  $\delta(V - I)_G$  versus  $\delta(B - V)_D$  is more ambiguous.

The colour residuals from Figure 5 are plotted versus the reddening from Reed et al. (1988) in Figure 6, the symbols being the same as in previous figures. There seems to be no correlation between  $E(B - V)_{\text{RHS88}}$  and either the  $\delta(B - V)_D$  residual (a Spearman test gives a two-tailed  $p$ -value of 0.59; Pearson  $r = -0.006$ ), or  $\delta(U - B)_A$  (Spearman  $p = 0.98$ , Pearson  $r = -0.067$ ), with the possible exception of the two most-highly-reddened clusters. In the case of the  $\delta(V - I)_G$  residuals, the clusters with  $E(B - V)_{\text{RHS88}} > 0.6$  do seem to be systematically redder than would be expected from the least-squares fit (see Figure 6). The  $p$ -value from the Spearman rank correlation test of  $\delta(V - I)_G$  versus  $E(B - V)_{\text{RHS88}}$  is 0.046, on the verge of significance, although the Pearson  $r = 0.051$  does not indicate a correlation. In the following discussions we often restrict consideration of  $\delta(V - I)$  residuals to less-reddened systems.

<sup>2</sup> This coefficient takes a value of 0.0 if there is no correlation between two variables, and values of +1 and -1 for perfect positive and negative correlations respectively.

**Table 2.** Pearson correlation coefficients  $r$ 

Correlation	Sample	$r$
$\delta(U - B)_A$ vs $B_T$	fit A; no [Fe/H] or $E(B - V)$ restrictions; 42 clusters	-0.432
$\delta(U - B)_C$ vs $B_T$	[Fe/H] < -0.5 and $E(B - V) < 0.5$ ; fit C; 41 clusters	-0.456
$\delta(U - B)_A$ vs $(B - V)_p$	fit A; no [Fe/H] or $E(B - V)$ restrictions; 42 clusters	0.156
$\delta(U - B)_C$ vs $(B - V)_p$	[Fe/H] < -0.5 and $E(B - V) \leq 0.5$ ; fit C; 41 clusters	0.015
$\delta(U - B)_C$ vs $\log \rho_0$	[Fe/H] < -0.5 and $E(B - V) \leq 0.5$ ; fit C; 72 clusters	-0.110
$\delta(U - B)_C$ vs $c$	[Fe/H] < -0.5, $E(B - V) \leq 0.5$ , $c < 2.0$ ; fit C; 57 clusters	-0.019
$\delta(U - B)_C$ vs $b/a$	[Fe/H] < -0.5 and $E(B - V) \leq 0.5$ ; fit C; 71 clusters	-0.197
$\delta(B - V)_D$ vs $B_T$	fit D; no [Fe/H] or $E(B - V)$ restrictions; 42 clusters	0.006
$\delta(B - V)_F$ vs $B_T$	[Fe/H] < -0.5 and $E(B - V) \leq 0.5$ ; fit F; 41 clusters	-0.004
$\delta(B - V)_D$ vs $(B - V)_p$	fit D; no [Fe/H] or $E(B - V)$ restrictions; 42 clusters	0.406
$\delta(B - V)_F$ vs $(B - V)_p$	[Fe/H] < -0.5 and $E(B - V) \leq 0.5$ ; fit F; 41 clusters	0.267
$\delta(B - V)_F$ vs $\log \rho_0$	[Fe/H] < -0.5 and $E(B - V) \leq 0.5$ ; fit F; 72 clusters	-0.264
$\delta(B - V)_F$ vs $c$	[Fe/H] < -0.5, $E(B - V) \leq 0.5$ , $c < 2.0$ ; fit F; 57 clusters	-0.089
$\delta(B - V)_F$ vs $b/a$	[Fe/H] < -0.5 and $E(B - V) \leq 0.5$ ; fit F; 71 clusters	-0.230
$\delta(V - I)_G$ vs $B_T$	fit G; no [Fe/H] or $E(B - V)$ restrictions; 42 clusters	-0.182
$\delta(V - I)_I$ vs $B_T$	$E(B - V) \leq 0.3$ ; fit I; 34 clusters	-0.293
$\delta(V - I)_G$ vs $(B - V)_p$	fit G; no [Fe/H] or $E(B - V)$ restrictions; 42 clusters	0.185
$\delta(V - I)_I$ vs $(B - V)_p$	$E(B - V) \leq 0.3$ ; fit I; 34 clusters	0.016
$\delta(V - I)_I$ vs $\log \rho_0$	$E(B - V) \leq 0.3$ ; fit I; 49 clusters	-0.164
$\delta(V - I)_I$ vs $c$	$E(B - V) \leq 0.3$ ; fit I; 49 clusters	-0.156
$\delta(V - I)_I$ vs $c$	$E(B - V) \leq 0.3$ and $c < 2.0$ ; fit I; 38 clusters	-0.323
$\delta(V - I)_I$ vs $b/a$	$E(B - V) \leq 0.3$ ; fit I; 49 clusters	0.079
$\delta(B - I)_K$ vs $B_T$	[Fe/H] < -0.5 and $E(B - V) \leq 0.5$ ; fit K; 41 clusters	-0.325
$\delta(B - I)_K$ vs $B_T$	[Fe/H] < -0.5, $E(B - V) \leq 0.5$ , $B_T < 9.5$ ; fit K; 36 clusters	-0.286
$\delta C_0(42 - 45)$ vs $B_T$	fit a; no [Fe/H] or $E(B - V)$ restrictions; 43 clusters	-0.013
$\delta C_0(42 - 45)$ vs $(B - V)_p$	fit a; no [Fe/H] or $E(B - V)$ restrictions; 43 clusters	0.210
$\delta C_0(42 - 45)$ vs $(B - V)_p$	fit a; 40 clusters (excludes NGC 288, NGC 4147, NGC 5694)	0.117
$\delta C_0(42 - 45)$ vs $\log \rho_0$	fit a; no [Fe/H] or $E(B - V)$ restrictions; 88 clusters	0.027
$\delta C_0(42 - 45)$ vs $c$	fit a; no [Fe/H] or $E(B - V)$ restrictions; 88 clusters	-0.142
$\delta C_0(42 - 45)$ vs $b/a$	fit a; no [Fe/H] or $E(B - V)$ restrictions; 85 clusters	-0.074
$\delta C_0(38 - 42)$ vs $B_T$	fit b; no [Fe/H] or $E(B - V)$ restrictions; 34 clusters	-0.543
$\delta C_0(38 - 42)$ vs $(B - V)_p$	fit b; no [Fe/H] or $E(B - V)$ restrictions; 34 clusters	-0.074
$\delta C_0(38 - 42)$ vs $\log \rho_0$	fit b; no [Fe/H] or $E(B - V)$ restrictions; 58 clusters	0.016
$\delta C_0(38 - 42)$ vs $c$	fit b; no [Fe/H] or $E(B - V)$ restrictions; 58 clusters	0.007
$\delta C_0(38 - 42)$ vs $b/a$	fit b; no [Fe/H] or $E(B - V)$ restrictions; 58 clusters	0.146
$\delta C_0(35 - 38)$ vs $B_T$	fit c; no [Fe/H] or $E(B - V)$ restrictions; 32 clusters	0.163
$\delta C_0(35 - 38)$ vs $B_T$	$E(B - V) \leq 0.3$ ; fit d; 26 clusters	0.101
$\delta C_0(35 - 42)$ vs $B_T$	fit e; no [Fe/H] or $E(B - V)$ restrictions; 32 clusters	-0.292
$\delta(C - T_1)_0$ vs $B_T$	full sample (31 clusters)	-0.099
$\delta(C - T_1)_0$ vs $(B - V)_p$	full sample (31 clusters)	0.361
$\delta(C - T_1)_0$ vs $(B - V)_p$	excluding NGC 288, NGC 6218, NGC 6402 (28 clusters)	0.203
$\delta(C - T_1)_0$ vs $\log \rho_0$	51 clusters	0.069
$\delta(C - T_1)_0$ vs $c$	51 clusters	0.071
$\delta(C - T_1)_0$ vs $b/a$	50 clusters	0.027
$\delta(C - M)_0$ vs $B_T$	full sample (31 clusters)	-0.180
$\delta(C - M)_0$ vs $B_T$	excluding NGC 288, NGC 6218, NGC 6402 (28 clusters)	-0.266
$\delta(C - M)_0$ vs $(B - V)_p$	full sample (31 clusters)	0.361
$\delta(C - M)_0$ vs $(B - V)_p$	excluding NGC 288, NGC 6218, NGC 6402 (28 clusters)	0.196
$\delta(M - T_1)_0$ vs $B_T$	full sample (31 clusters)	-0.031
$\delta(M - T_1)_0$ vs $(B - V)_p$	full sample (31 clusters)	0.331
$\delta(M - T_1)_0$ vs $(B - V)_p$	excluding NGC 288, NGC 6218, NGC 6402 (28 clusters)	0.189

**Table 3.** Colour residuals for some example clusters

Cluster	[Fe/H]	HB <sup>1,2</sup>	$\delta(U-B)_A$	$\delta(U-B)_B$	$\delta(B-V)_D$	$\delta(B-V)_E$	$\delta(V-I)_G$	$\delta(V-I)_I$	$\delta(B-I)_K$
NGC 1851	-1.23	B	0.00	-0.01	0.03	0.02	0.03	0.02	0.04
NGC 2808	-1.36	B,G	-0.04	-0.05	-0.02	-0.02	-0.07	-0.07	-0.13
NGC 4590	-2.11	G	0.02	0.02	-0.02	-0.01	0.01	0.05	0.07
NGC 5272	-1.66		0.01	0.01	0.02	0.03	0.00	0.02	0.05
NGC 6121	-1.27	B	-0.06	-0.07	-0.09	-0.09	0.01	....	-0.15
NGC 6205	-1.63	G	-0.11	-0.11	0.00	0.00	-0.09	-0.08	-0.18
NGC 6229	-1.54	B,G	-0.14	-0.14	0.01	0.01	0.06	0.07	-0.06
NGC 6341	-2.24	G	0.04	0.05	0.03	0.04	0.01	0.05	0.15
NGC 6362	-1.18	B,	0.05	0.04	0.08	0.08	0.07	0.06	0.18
NGC 6388	-0.74	B,G	0.02	0.01	0.00	-0.01	-0.02	....	-0.05
NGC 6441	-0.59	B,G	0.02	0.00	-0.02	-0.03	-0.01	....	-0.08
NGC 6638	-1.00	G	-0.02	-0.03	0.00	-0.01	0.01	....	-0.04
NGC 6681	-1.64	G	-0.03	-0.03	-0.02	-0.02	-0.03	-0.01	-0.06
NGC 6712	-1.07	B	-0.04	-0.05	-0.01	-0.02	0.04	....	-0.05
NGC 6723	-1.12	B	0.00	-0.01	-0.01	-0.01	0.03	0.02	0.00
NGC 6752	-1.54	G	-0.06	-0.06	-0.05	-0.05	-0.05	-0.04	-0.15
NGC 6809	-1.80	G	0.00	0.01	-0.02	-0.09	0.02	0.04	0.04
NGC 6864	-1.32	B	0.01	0.00	0.02	0.02	0.03	0.02	0.04
NGC 7006	-1.59		-0.08	-0.08	-0.01	0.00	-0.02	-0.01	-0.09
NGC 7078	-2.13	G	0.02	0.03	0.01	0.03	-0.11	-0.07	-0.01

<sup>1</sup> B: denotes a cluster with a bimodal HB, i.e., a deficiency of RR Lyrae stars but well-populated blue and red horizontal branches.

<sup>2</sup> G: a cluster having a gap in the colour distribution of the blue horizontal branch stars.

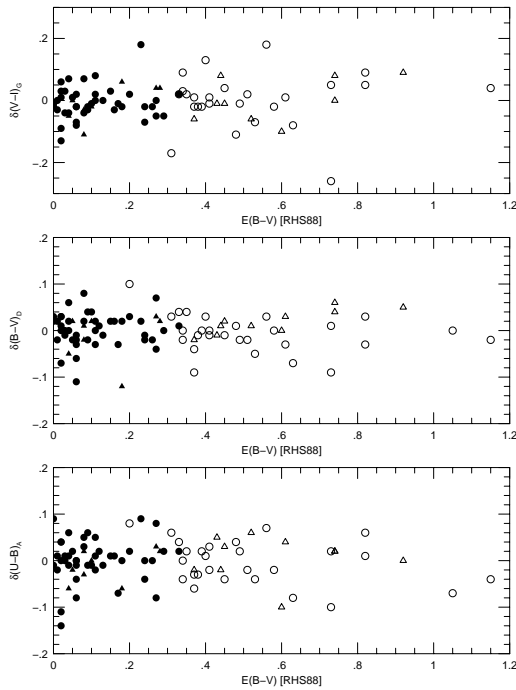


**Fig. 6.** The colour residuals from Figure 5 are shown versus cluster reddening from Reed et al. (1988; RHS88). The residuals are with respect to the colour-metallicity fits listed as A, D, and G in Table 1. Symbols are the same as for Figures 1 and 2.

In an effort to obtain some measure of the uncertainty in the reddenings of each cluster in the combined MV68 and BP83 samples, we calculated the differences  $\Delta E(B-V)$  between the reddening values from RHS88 and H99. The values of  $\Delta E(B-V)$  fall in the range  $-0.05$  to  $0.10$  for all but three clusters in the MV68+BP83 sample. Spearman rank correlation tests between  $\Delta E(B-V)$  and the colour residuals from Figure 6 were performed. These yielded  $p$ -values of  $0.49$ ,  $0.08$ , and  $0.195$  for  $\delta(U-B)_A$ ,  $\delta(B-V)_D$ , and  $\delta(V-I)_G$  respectively. With the possible exception of a few clusters, there is no significant evidence from the Spearman test for any correlation between the *UBVI* colour residuals and uncertainties in reddening.

The data presented in Figures 5 and 6, together with the statistical tests noted above, therefore give somewhat ambivalent indications as to whether errors in measured cluster reddenings have a serious effect on the residuals about the *UBVI* colour-metallicity relations of Figures 1-4. This complicating effect will add scatter to any correlations we are searching for between these colour residuals and the horizontal branch morphology of globular clusters. In many of the discussions below we will accordingly conduct tests using both the largest available sample of clusters, as well as samples restricted by reddening.

## 2.4. *UBVI* Colour Residuals for Some Example Clusters

As noted above, one expected influence on integrated colours of globular clusters is the morphology of the horizontal branch. Values of *UBVI* colour residuals are listed in Table 3 for some clusters with notable HB morphologies. The pair of clusters M3 (NGC 5272) and M13 (NGC 6205) consti-

tute a classic example of the second-parameter phenomenon (e.g., Catelan & de Freitas Pacheco 1995). Although they have very similar [Fe/H] abundances they differ in horizontal branch morphology, with M13 having a more extensive blue horizontal branch that extends to a  $V$  magnitude comparable to the main sequence turnoff (Johnson & Bolte 1998; Rey et al. 2001). By contrast, NGC 7006 is similar to both M3 and M13 in metallicity, but has a much larger fraction of HB stars on the red side of the RR Lyrae gap (Sandage & Wildey 1967; Buonanno et al. 1991). It is again a classic example of a second-parameter phenomenon.

In addition to the second-parameter triplet of M3-M13-NGC7006, *UBVI* colour residuals are listed in Table 3 for other GCs having non-uniform horizontal branches. Even more extreme than the HB of M13 is that of NGC 2808, which not only extends to a  $V$  magnitude below the main sequence turnoff, but has a deficiency of RR Lyrae variables and yet a well-populated red HB (Harris 1974; Walker 1999; Bedin et al. 2000). As such, this cluster is said to have a “bimodal” HB. In addition, there are other “gaps” in the colour distribution along the blue HB. NGC 6229 is another such bimodal HB cluster like NGC 2808; these clusters constitute two of the cases in which gaps occur in the HB colour distribution both in the RR Lyrae region as well as along the BHB (Catelan et al. 1998). NGC 6752 is a cluster that is known for an extended blue horizontal branch having considerable structure (e.g., Newell & Sadler 1978, Buonanno et al. 1986, Momany et al. 2002). Both NGC 6388 and NGC 6441 are examples of GCs with relatively high metallicities yet a population of blue HB stars (Rich et al. 1997; Moehler, Sweigart, & Catelan 1999). They are classified as being both “bimodal” and “gap” HB clusters by Catelan et al. (1998). Other GCs classified by Catelan et al. (1998) as having either bimodal or gap HB morphologies are also listed in Table 3; these being identified by either the letter B or G in column 3.

Are there clusters in Table 3 having integrated-colour residuals that might be attributed to the effect of a very blue horizontal branch? Possibly. Relative to M3 the extended-BHB cluster M13 has markedly bluer  $(U - B)_0$  and  $(B - I)_0$  colours, although the  $(B - V)_0$  colours of these two objects are very similar<sup>3</sup>. The bimodal and BHB-gap cluster NGC 6229 also has a  $(U - B)_0$  colour with a notable blue excess of  $\delta(U - B)_{A,B} = -0.14$ , although like M13, the  $\delta(B - V)$  residual is not significantly different from zero. Oddly enough, NGC 7006 has an integrated  $(U - B)_0$  colour that is only slightly redder than that of M13 despite the considerable difference in their HB structures. This can be seen from the similar values of  $\delta(U - B)_{A,B}$  for these clusters (Table 3). Noted for an extended BHB is NGC 6752, which does exhibit consistent blue excesses in all of the *UBVI* colours (Table 3), as may NGC 2808. However, many of the clusters in Table 3 have colour residuals that do not depart significantly from zero, despite some notable properties to their horizontal branches. In the next section we look at possible

connections between HB morphology and integrated colour in a more systematic way.

## 2.5. Correlations Between *UBVI* Colour Residuals and Horizontal Branch Morphology

Several parameters have been used in the literature to reflect the morphology of the horizontal branch. Two quantities, which we denote as  $(B - V)_p$  and  $B_T$ , were introduced by Fusi Pecci et al. (1993). The first of these parameters,  $(B - V)_p$ , refers to the dereddened colour at which the density of stars along the locus of the HB in a  $V, (B - V)_0$  colour-magnitude diagram reaches a maximum. The second quantity is designed to reflect the extent of the blue horizontal branch. Formally, Fusi Pecci et al. (1993) define  $B_T$  as “the length of the blue tail, measured along the ridge line of the HB starting from  $(B - V)_p$  down to the adopted blue HB extreme.” The parameter is measured along the locus of the HB, and seems to be normalised in such a way that it has the value 10.0 for the horizontal branch of Messier 3. Examples of how  $(B - V)_p$  and  $B_T$  are defined can be found in Figure 3 of Fusi Pecci et al. (1993). The  $B_T$  parameter shows a wide dispersion at a given [Fe/H], particularly among intermediate-metallicity clusters. As discussed by Fusi Pecci et al. (1993), this parameter can be used to study the systematics of second-parameter effects involving HB stars on the blue side of the RR Lyrae region. By contrast,  $(B - V)_p$  is more nearly correlated with [Fe/H], although it still exhibits substantial scatter at a given metallicity indicative of second-parameter effects, particularly among clusters with [Fe/H]  $\sim -1.5$ .

Two sets of  $\delta(U - B)$  residuals are plotted versus HB parameters in Figures 7 and 8. Separate panels in each figure show residuals computed for the full sample of clusters (identified with fit A in Table 1), and for the subset restricted to  $E(B - V)_{H99} \leq 0.5$  and [Fe/H]  $< -0.5$  (identified with fit C). There does appear to be a relation between  $\delta(U - B)$  residuals and  $B_T$ , albeit with considerable scatter. If the unrestricted sample of clusters is considered, then the Pearson linear correlation coefficient between  $B_T$  and the  $\delta(U - B)_A$  residuals is  $r = -0.43$  (Table 2). There are 42 clusters in this sample for which values of  $B_T$  are available. The correlation coefficient is little different ( $r = -0.46$  for 41 clusters) if the analysis is based on those GCs from the upper panel of Figure 7 together with fit C from Table 1. By contrast to these trends with  $B_T$ , Figure 8 shows little if any correlation between  $\delta(U - B)$  and  $(B - V)_p$ , which is confirmed by the  $r$ -values listed in Table 2.

In the case of the  $B - V$  residuals there is little evidence for a relation with the  $B_T$  parameter, as the correlation coefficients in Table 2 indicate. This would suggest that  $B - V$  is less susceptible to an extended blue HB morphology than  $U - B$ . By contrast, however, there may be a hint of some link between residuals in  $(B - V)_0$  and the modal HB colour  $(B - V)_p$ , as illustrated in Figure 9. Adopting fit D from Table 1 and the full sample of clusters, the Pearson correlation coefficient between  $\delta(B - V)_D$  and  $(B - V)_p$  is  $r = 0.41$  (Table 2). However, if instead we consider just those clusters of restricted reddening and [Fe/H] for which fit F of Table 1 applies, then the resulting  $\delta(B - V)_F$  residuals and  $(B - V)_p$

<sup>3</sup> In the case of M13  $(U - B)_0 = -0.03$ ,  $(B - I)_0 = 1.46$ , and  $(B - V)_0 = 0.66$ , with equivalent colours of 0.08, 1.68, and 0.68 for M3.



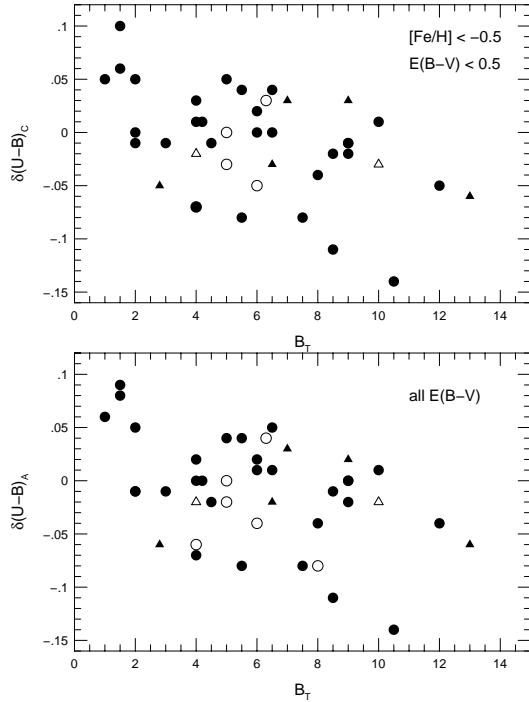


**Fig. 7.** Two sets of  $\delta(U - B)$  residuals versus the horizontal branch parameter  $B_T$ . The bottom panel shows residuals relative to the linear fit A from Table 1, which is based on all clusters in the present sample except NGC 6316. In the top panel the residuals are measured with respect to a linear colour-metallicity relation based on the subset of clusters for which  $E(B - V)_{\text{H99}} \leq 0.5$  and  $[\text{Fe}/\text{H}] < -0.5$  (fit C of Table 1). Values of  $B_T$  are not available for all of the clusters on which fits A and C are based. Symbols have the same meaning as in Figure 2.

have a lower correlation coefficient of  $r = 0.27$ . Thus, the evidence for any relation between  $(B - V)_0$  excess and HB morphology is sensitive to how the cluster sample is restricted with respect to reddening. Five of the six clusters in Figure 9 that have colour excesses of  $\delta(B - V)_{\text{D,F}} < -0.05$  do have relatively blue modal HB colours of  $(B - V)_p \leq 0.2$ . Thus, there may be a small subset of GCs whose  $(B - V)_0$  colours show a second-parameter effect. If  $\delta(B - V)$  does have some correlation with  $(B - V)_p$  but not  $B_T$ , then it may imply either that  $B - V$  is more sensitive to the mean HB colour than to the colour distribution of extended blue-tail stars, or that a first-order fit to the  $(B - V)_0$  versus  $[\text{Fe}/\text{H}]$  relation is not quite adequate.

Since the sensitivity of  $(B - V)_p$  to second-parameter effects is most apparent among intermediate-metallicity clusters, Figure 10 shows the  $\delta(B - V)_E$  residuals (relative to fit E) versus both HB parameters for clusters in the metallicity range  $-1.8 \leq [\text{Fe}/\text{H}] \leq -1.3$ . The residuals in this case are relative to the colour-metallicity relation based on clusters with  $E(B - V)_{\text{H99}} < 0.5$ , but with no restriction on  $[\text{Fe}/\text{H}]$ .

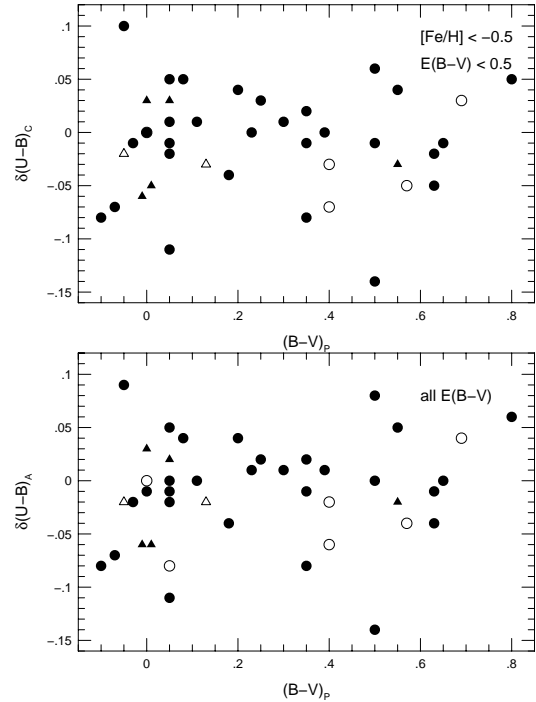


**Fig. 8.** Two sets of  $\delta(U - B)$  residuals versus the horizontal branch parameter  $(B - V)_p$ . Other details are the same as for Figure 7. Residuals are relative to colour-metallicity fits A and C from Table 1. Symbols have the same meaning as in Figure 2.

There is no correlation with  $B_T$ , as found for the full cluster sample. In the case of any correlation with  $(B - V)_p$ , Figures 9 and 10 show that this seems to be evinced by only a small number of clusters with relatively blue HB modal colours. All but four GCs in Figure 10 have  $|\delta(B - V)_E| \leq 0.03$ , with the four most anomalous clusters having  $(B - V)_p \leq 0.2$ . Thus, among the intermediate-metallicity GCs, the second-parameter effect on integrated  $(B - V)_0$  again seems to be limited to a small fraction of objects whose modal HB colour is fairly blue, although the values of  $B_T$  for these clusters are not extreme (see the lower panel of Figure 10).

Sil'chenko (1983) used colour-magnitude diagrams of Milky Way globular clusters from the Dudley catalogue (Philip, Cullen, & White 1976) to compute the fraction of integrated cluster light in the  $UBV$  passbands that is contributed by the horizontal branch population. One finding from this work was that for clusters of metallicity  $[\text{Fe}/\text{H}] < -1.1$  the change in  $B - V$  colour induced by subtracting out the horizontal branch stars is “independent of the intrinsic horizontal-branch color,” although it does scale with the percentage contribution of HB stars to the integrated  $V$  magnitude. In other words, the effect of HB stars on the integrated  $B - V$  colour was found to vary directly with the relative number of HB stars in a cluster, but was less sensitive to their colour distribution. Sil'chenko's (1983) findings

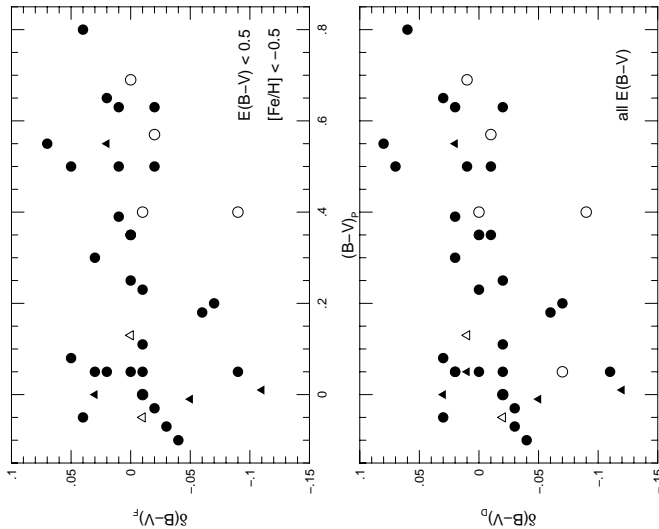


**Fig. 9.** Two sets of  $\delta(B - V)$  residuals versus the horizontal branch parameter  $(B - V)_p$ . The bottom panel shows residuals relative to the linear fit D from Table 1. In the top panel the residuals are measured with respect to a linear colour-metallicity fit based on clusters for which  $E(B - V)_{\text{H99}} \leq 0.5$  and  $[\text{Fe}/\text{H}] < -0.5$  (fit F of Table 1). Symbols have the same meaning as in Figure 1.

may accord with the lack of any strong correlation between  $\delta(B - V)$  and  $B_T$ , although the most discrepant clusters in Figures 9 and 10 may provide exceptions.

Two sets of  $\delta(V - I)$  residuals are plotted against  $B_T$  in Figure 11. There appears to be only weak evidence for a correlation. In the top panel there may be a very weak trend with considerable scatter between  $\delta(V - I)_I$  (relative to fit I) and  $B_T$  for clusters with  $E(B - V)_{\text{H99}} < 0.3$  ( $r = -0.29$ ; Table 2). However, this is not evident for the full sample of GCs unrestricted by reddening (bottom panel). There is no evidence of a correlation between the  $\delta(V - I)$  residuals and  $(B - V)_p$ , as the correlation coefficients in Table 2 demonstrate.

Could the lack of a correlation between  $\delta(B - V)$  residuals and  $B_T$  be due to comparable sensitivities of the integrated  $B$  and  $V$  magnitudes to extended blue horizontal branch morphology? If the  $B$  magnitude is affected by a long BHB tail then it may be more apparent in the  $(B - I)_0$  colour, since the  $I$  band samples less of the flux from BHB stars than the  $V$  band. The  $\delta(B - I)$  residuals about the colour-metallicity fits in Figure 4 are plotted versus the horizontal branch parameter  $B_T$  in Figure 12. Among clusters with  $B_T < 7$  there is basically a random scatter in  $\delta(B - I)$ , while among those relatively few clusters with  $B_T > 7$  there may

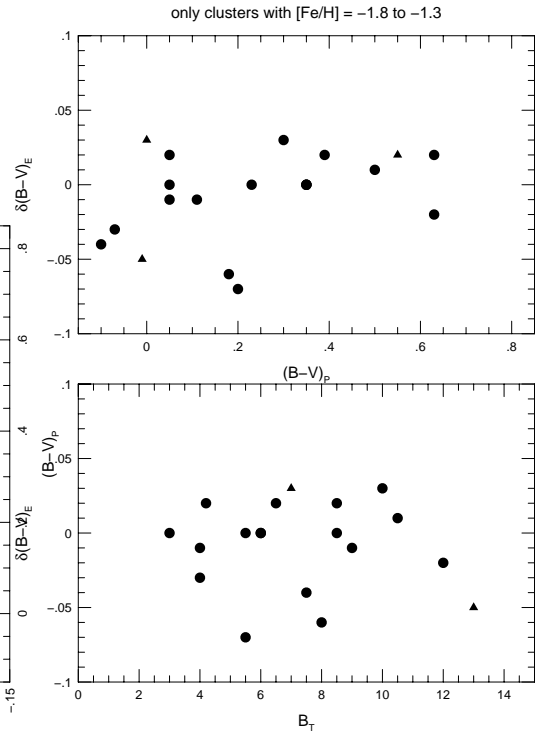


**Fig. 10.** The  $\delta(B - V)_E$  residual versus both horizontal branch parameters  $B_T$  and  $(B - V)_p$ . The residuals are measured with respect to fit E from Table 1, and only clusters in the restricted metallicity range  $-1.8 \leq [\text{Fe}/\text{H}] \leq -1.3$  are shown. Symbols have the same meaning as in Figure 1.

be a trend to negative residuals, i.e., to bluer  $(B - I)_0$  colours than given by the least-squares fits. The Pearson correlation coefficient between  $B_T$  and  $\delta(B - I)_K$  for the clusters with  $[\text{Fe}/\text{H}] < -0.5$  and  $E(B - V)_{\text{H99}} < 0.5$  is  $r = -0.33$ ; if the sample is restricted to those clusters with  $B_T < 9.5$  the coefficient is  $r = -0.29$ . This is comparable to the value of  $r$  found for  $\delta(V - I)_I$  versus  $B_T$ . These results seem consistent with there being only a small influence of horizontal branch morphology on the  $B - I$  and  $V - I$  colours until an extended blue tail is developed.

## 2.6. Correlations with other Cluster Parameters?

### 2.6.1. Cluster Structure

Colour and stellar population gradients are found in some globular clusters. This is particularly the case with clusters having a high central concentration or a post-core-collapse morphology, wherein the integrated cluster starlight becomes bluer towards the center in an effect that “involves at least a few percent of the total visible light” (Djorgovski et al. 1991). These colour gradients appear to be due to diminished numbers of red giants near cluster center (e.g., Howell, Guhathakurta, & Tan 2000) possibly in combination with the presence of an inner population of stars that emits brightly

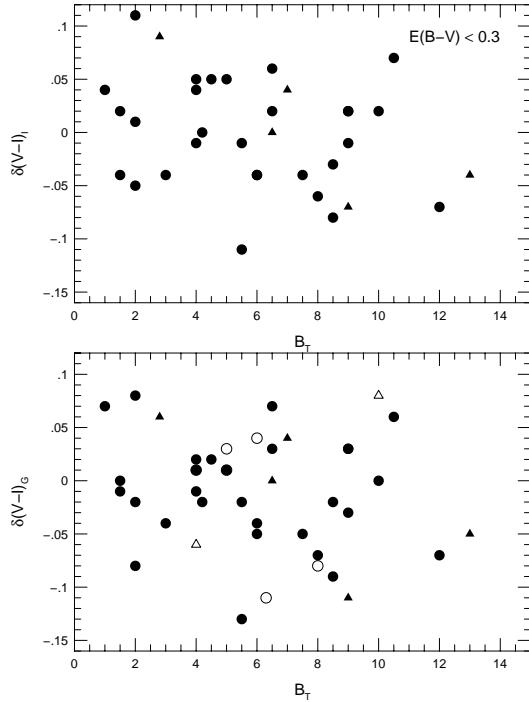


**Fig. 11.** Two sets of  $\delta(V - I)$  residuals versus the horizontal branch parameter  $B_T$ . In the top panel the residuals are measured with respect to a colour-metallicity relation based on the subset of clusters for which  $E(B - V)_{\text{H99}} \leq 0.3$  (fit I of Table 1). The bottom panel shows residuals relative to fit G, which is based on all clusters with  $V - I$  data regardless of reddening. Symbols have the same meaning as in Figures 1 and 2.

at ultraviolet wavelengths (Djorgovski et al. 1991; Djorgovski & Piotto 1992). Mass segregation effects could therefore influence integrated colours measured within the inner regions of a globular cluster. This suggests checking whether the colour residuals calculated in the previous section show any trend with the bulk physical properties of GCs.

We therefore tested for trends between the colour residuals  $\delta(U - B)_A$ ,  $\delta(B - V)_D$ , and  $\delta(V - I)_I$  (measured with respect to fits A, D, and I from Table 1), versus several “structure” parameters describing cluster mass, concentration, and shape. The parameters chosen were: (i) the central density  $\rho_0$  in units of  $L_\odot \text{pc}^{-3}$ , (ii) the concentration parameter  $c = \log r_t / r_c$ , values for both of these being obtained from H99, and (iii) an ellipticity parameter  $b/a$  measured by White & Shawl (1987), which is equal to the ratio of the lengths of the minor and major axes as determined from cluster isophotes. Correlation coefficients calculated in these tests are listed in Table 2. In the case of the  $UBV$  colour residuals there seem to be no discernible correlations with either  $\log \rho_0$ ,  $c$ , or  $b/a$ . Any  $UBV$  colour gradients that exist in core-collapse clusters do not seem to be detectable above the observational uncertainties in the integrated colours.

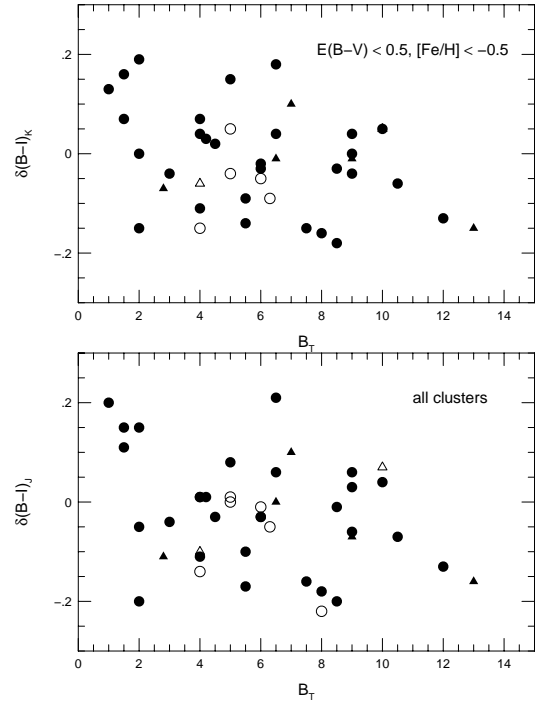


**Fig. 12.** Two sets of  $\delta(B - I)$  residuals versus the horizontal branch parameter  $B_T$ . The bottom panel shows results for the full sample of clusters with  $\delta(B - I)_J$  residuals relative to the colour-metallicity relation given by fit J. Symbols are the same as for Figure 1. In the top panel the residuals are measured with respect to fit K based on the subset of clusters for which  $E(B - V)_{\text{H99}} \leq 0.5$  and  $[\text{Fe}/\text{H}] \leq -0.5$ .

The  $\delta(V - I)_I$  residuals are shown plotted against the three GC morphology parameters in Figure 13, the symbols again denote both reddening and core structure as in previous plots. There may be some very modest trend with the concentration parameter  $c$ , in the sense that some clusters with  $c < 1.3$  are slightly redder in  $V - I$  than the mean colour-metallicity fit. However, among the core-collapse GCs there is a wide range in  $\delta(V - I)_I$ , with little propensity to the negative residuals that would be anticipated if the central regions of these clusters were depleted in red giants. For clusters with  $E(B - V)_{\text{H99}} < 0.3$  and  $c < 2.0$ , the central concentration  $c$  and the  $\delta(V - I)_I$  residuals have a Pearson correlation coefficient of  $r = -0.32$ . Thus, the  $V - I$  colour may show a marginal tendency to be redder in low-concentration clusters than in systems with  $c > 1.3$ . This could be consistent with some depopulation of the cores of high-concentration clusters in red giants. However, if such a phenomenon has occurred then it appears to be more detectable in  $V - I$  than in  $U - B$ , and it is curious that the integrated  $V - I$  colours of core-collapse clusters with  $c = 2.5$  do not show any anomalies. In summary, with the possible exception of the  $V - I$  residuals for low-reddening objects, there is little or no evi-

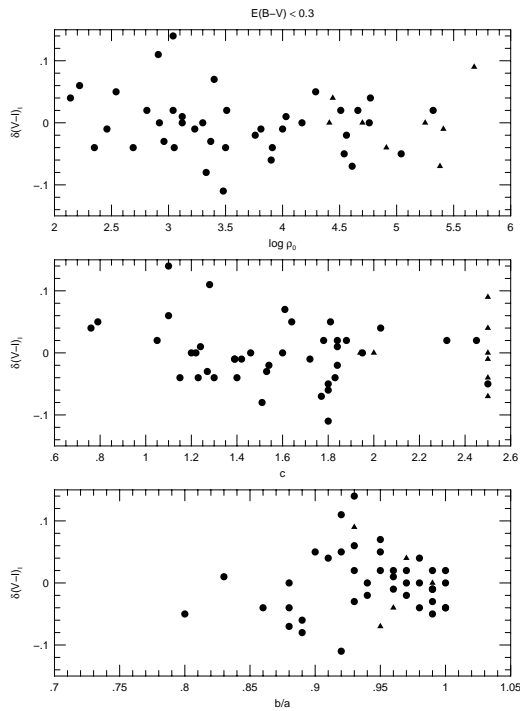


**Fig. 13.** The colour residual  $\delta(V - I)_I$  measured relative to fit I from Table 1 versus GC central luminosity density  $\log \rho_0$  ( $L_\odot \text{ pc}^{-3}$ ), concentration parameter  $c$ , and ellipticity parameter  $b/a$ . Symbols are the same as for Figure 1.

dence for any correlations between  $UBVI$  colour residuals and globular cluster structure.

### 2.6.2. Cluster Age

There is some evidence that for an age spread among Galactic globular clusters (e.g., Rosenberg et al. 1999). What effect might this have on our results? If age is strongly correlated with metallicity, then it should be accounted for in our initial colour-metallicity fits. However, if there is substantial scatter in cluster age at fixed metallicity, then age variations might be a factor in setting the colour residuals. To test for this, we have taken relative ages from De Angeli et al. (2005) for 49 clusters in common with our sample. The relative age is defined as the ratio between the measured age and a fiducial average for GCs with metallicities on the Zinn & West (1984) scale of  $[\text{Fe}/\text{H}] < -1.7$ . These clusters have a mean age of 11.2 Gyr. We performed Spearman rank correlation tests between the relative ages and both  $\delta(U - B)_A$  and  $\delta(B - V)_D$ , two colour residuals that show at least partial evidence for dependence on the horizontal branch parameters  $B_T$  and  $(B - V)_p$  respectively. The resulting two-tailed  $p$ -values are 0.87 and 0.04 respectively. The Pearson  $r$ -values were found to be 0.025 and  $-0.304$  respectively. These results indicate little or no evidence for a correlation in the case of the  $U - B$  residual. We conclude that age variations are

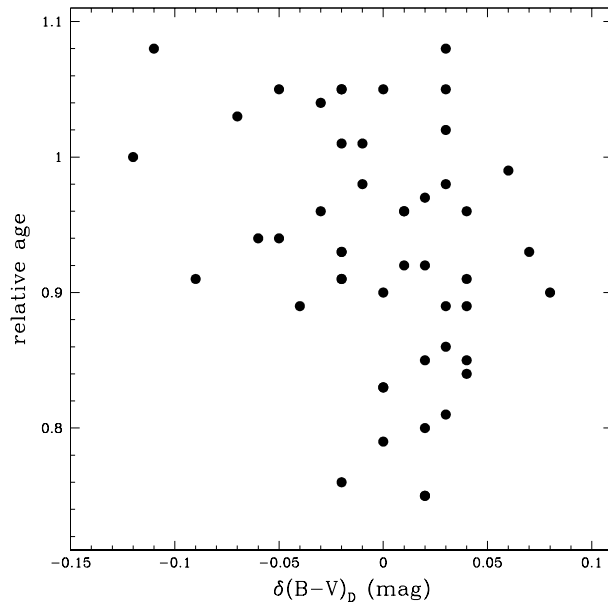


**Fig. 14.** Relative cluster age, referenced to a mean of 11.2 Gyr for metal-poor clusters with  $[\text{Fe}/\text{H}] < -1.7$ , versus the  $\delta(B - V)_D$  colour residual. The ages are from De Angeli et al. (2005).

unlikely to be responsible for the correlation found between the  $U - B$  residuals and  $B_T$ .

A plot of relative age versus the  $\delta(B - V)_D$  residual is shown in Figure 14. The  $p$ -value from the Spearman test for this residual may suggest a marginal correlation, as may the Pearson  $r$ -value. Inspection of Figure 14 indicates that this result may be weighted by a small subset of clusters with colour residuals of  $\delta(B - V)_D < -0.05$  and relative ages greater than 0.9. Such clusters also have fairly blue HB  $(B - V)_p$  colours, as seen in Figures 9 and 10. Thus it may be difficult to disentangle an age from a second-parameter HB effect for these clusters. Any interpretation is further complicated by the fact that the relative ages of De Angeli et al. (2005) are dependent on the magnitude difference between main sequence turnoff and horizontal branch stars, and so could be subject to second-parameter effects.

## 3. DDO Colours

Integrated photometry is also available for Milky Way globular clusters in the intermediate-band DDO filters. This system is well known to be useful for deriving photometric effective temperatures, gravities and metallicities of late-type stars, particularly red giants (e.g., Osborn 1973; Janes 1975; Sung & Lee 1987; Claria et al. 1994a; Claria, Piatti, & Lapasset 1994b). On account of the lower count levels with the DDO filters due to their narrower bandpasses and transmission in the violet region of the spectrum, integrated-light studies with this filter system have only been made to date for the Milky Way and M31 globular cluster systems.

Integrated DDO colours of Milky Way GCs have been measured by McClure & van den Bergh (1968) and Bica

& Pastoriza (1983). The former observers used one or two-channel photometers having 1P21 photomultiplier tubes on the David Dunlap Observatory 1.9-m and Cerro Tololo Inter-American Observatory 0.4-m telescopes. Bica & Pastoriza (1983) used a “photon counter device, equipped with an EMI9658 RAM photomultiplier” on the 0.5-m telescope of the Universidade Federal do Rio Grande do Sul. The DDO system incorporates five colours. The three more usual ones are denoted  $C(45-48)$ ,  $C(42-45)$  and  $C(41-42)$ . The first of these was only measured for Milky Way GCs by BP83, while both MV68 and BP83 give values of  $C(42-45)$  and  $C(41-42)$ . The  $C(42-45)$  colour is the main effective temperature indicator in the DDO system, and was confirmed to be sensitive to cluster metallicity in integrated light by BP83 and Brodie & Huchra (1990). In addition, MV68 measured two other colours:  $C(38-41)$  and  $C(35-38)$ . The first of these is sensitive to the Ca II H&K break which is a known metallicity discriminator for galaxies. The second of these straddles the Balmer series break, with both the  $C38$  and  $C35$  filter bandpasses containing strong hydrogen lines. Brodie & Huchra (1990) looked at the correlations between  $[\text{Fe}/\text{H}]$  and the integrated DDO colours  $C(38-41)$ ,  $C(38-42)$ ,  $C(41-42)$ , and  $C(42-45)$  using the data of McClure & van den Bergh (1968) for Milky Way globular clusters. They did not attempt to correct these colours for interstellar reddening.

McClure & van den Bergh (1968) made multiple observations of many clusters, and their Table VI lists for each such object the average deviation of the individual measurements from the mean. These deviations vary considerably, being 0.02-0.03 in all colours for many clusters, but as large as 0.06-0.10 for others. A comparison can be made between the measurements of MV68 and BP83 for the  $C(42-45)$  colour. The mean value of the difference  $\Delta C(42-45)$  [BP83-MV68] is 0.010 mag with a standard deviation of 0.033 mag for the 64 clusters reported in both papers. We found no evidence that this difference varies with cluster metallicity, with the Pearson correlation coefficient between  $\Delta C(42-45)$  and  $[\text{Fe}/\text{H}]$  being  $r = 0.153$  for 64 clusters.

Observed colours were corrected for reddening using the  $E(B-V)$  values from the H99 catalog, and adopting the standard reddening ratios of McClure & van den Bergh (1968) and McClure (1973). Interstellar reddening in all of the DDO colours is small compared with  $E(B-V)$ . Given also the narrower DDO filter bandpasses and smaller wavelength separation, the reddening ratios between DDO colours should show less of a variation with cluster spectral type than the  $UBVI$  colours. We use the colour  $C_0(38-42)$  rather than  $C_0(38-41)$  throughout this paper. The  $C41$  filter bandpass contains the  $\lambda 4215$  CN band, and since CN inhomogeneities are common within Milky Way GCs we try to avoid this possible complication on the integrated colours. Nonetheless, the flux in the  $C42$  filter is sensitive to the carbon abundance via the strength of the  $\lambda 4300$  G band (Bell, Dickens, & Gustafsson 1979; Tripicco & Bell 1991).

The most metallicity-sensitive of the standard DDO colours are  $C_0(42-45)$  and  $C_0(38-42)$ . Figures 15 and 16 show these colours versus  $[\text{Fe}/\text{H}]$ . In both cases linear least-

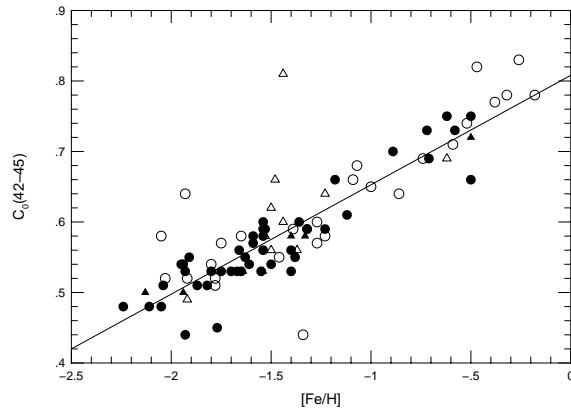


**Fig. 15.** The integrated  $C_0(42-45)$  colours of Milky Way globular clusters versus metallicity. A linear least-squares fit (labelled  $a$  in Table 1) is shown. As with Figure 1, triangles denote core-collapse clusters, while filled and open symbols correspond to clusters with reddenings of  $E(B-V)_{\text{H99}} \leq 0.3$  and  $E(B-V)_{\text{H99}} > 0.3$  respectively. The three most discordant clusters in the figure were not included in the determination of the linear fit.

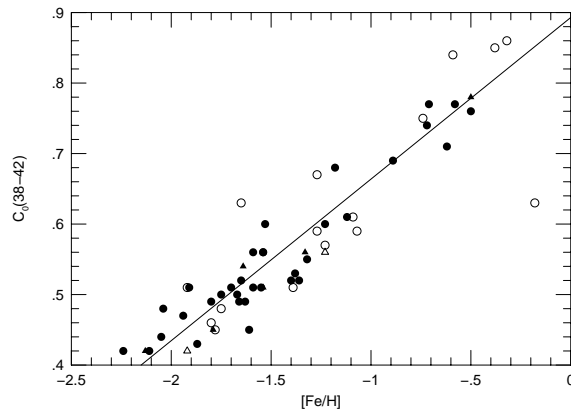


**Fig. 16.** The integrated  $C_0(38-42)$  colours of Milky Way globular clusters versus metallicity. A linear least-squares relation is shown, the coefficients for which are listed as fit  $b$  in Table 1. The discordant point for cluster NGC 6553 was not included in the fit. Symbols are the same as for Figures 1 and 15.

squares fits are shown as solid lines; they appear to match the observed correlations quite well. Coefficients of these fits are listed in Table 1 (fits  $a$  and  $b$ ). The cluster NGC 6553 was not included in the determination of the fit between  $C_0(38-42)$  and  $[\text{Fe}/\text{H}]$ , the point for this system being far removed from the mean trend in Figure 16. In the case of the  $C_0(42-45)$  colour there are several clusters (NGC 6144, NGC 6325, and NGC 6517) which fall well away from the main trend in Figure 15, and these have been omitted in determining the fit coefficients listed in Table 1. There are a number of clusters

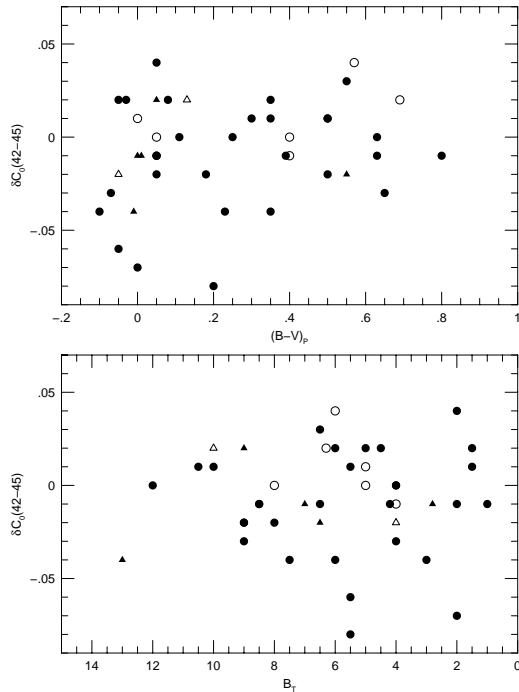


**Fig. 17.** The  $\delta C_0(42 - 45)$  residuals about the linear fit  $a$  shown in Figure 15 versus the horizontal branch parameters  $B_T$  and  $(B - V)_p$ . Symbols have the same meaning as for Figure 1.

for which MV68 did not measure a  $C(42 - 45)$  colour, such that the plotted values are based entirely on the measurements of BP83. NGC 6144, NGC 6325, and NGC 6517 are three such clusters, and so without comparison observations, it is not clear whether their discordant positions in Figure 15 can be attributed to observational error.

The  $\delta C_0(42 - 45)$  residuals with respect to fit  $a$  are shown versus both horizontal branch parameters  $B_T$  and  $(B - V)_p$  in Figure 17. There is no obvious correlation with the former of these indices, as confirmed by the Pearson  $r$ -value in Table 2. Also, with the possible exception of the three clusters with  $\delta C_0(42 - 45) < -0.05$  (NGC 288, NGC 4147, and NGC 5694), there is no correlation of this colour excess with  $(B - V)_p$ . All three of these clusters have  $(B - V)_p < 0.25$ . However, many other globulars with similar HB modal colours are not abnormally blue in  $C_0(42 - 45)$ . In addition, these three clusters do not have extended BHB tails (they all have  $B_T < 6.0$ , see the lower panel of Figure 17). Given that all three objects lack photometry from McClure & van den Bergh (1968), we feel that no compelling case can be made for a dependence of the  $C_0(42 - 45)$  colour on horizontal branch morphology. The Pearson coefficients in Table 2 show that there are no correlations between the  $\delta C_0(42 - 45)$  residuals and any of the cluster structure parameters  $\log \rho_0$ ,  $c$ , or  $b/a$ .

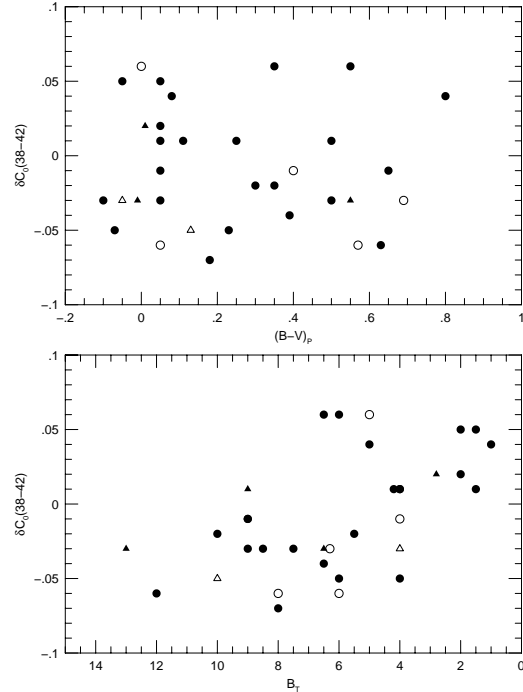


**Fig. 18.** The  $\delta C_0(38 - 42)$  residuals about the linear fit  $b$  from Table 1 (see also Figure 16) versus the horizontal branch parameters  $B_T$  and  $(B - V)_p$ . Symbols have the same meaning as for Figure 1.

Plots analogous to those of Figure 17, but for the residual  $\delta C_0(38 - 42)$ , are shown in Figure 18. The colour-metallicity relation for  $C_0(38 - 42)$  reveals that this is a more sensitive  $[\text{Fe}/\text{H}]$  diagnostic than  $C_0(42 - 45)$  for integrated light. The  $\delta C_0(38 - 42)$  residual shows little trend with  $(B - V)_p$  ( $r = -0.07$ ), but it does exhibit a correlation, albeit with considerable scatter, with the blue-tail parameter  $B_T$  ( $r = -0.54$ , Table 2). There is no evidence for any relation between  $\delta C_0(38 - 42)$  and either GC central density, concentration, or ellipticity (Table 2).

As noted above, the  $C_0(35 - 38)$  colour measures the strength of the Balmer jump. Consequently, it is sensitive to both stellar effective temperature and surface gravity. Within stars of the same luminosity class, this colour increases in value from spectral type B0 through A0, and then becomes more negative along a sequence from A through mid-K stars. Among A through M stars it increases in value as the luminosity class changes from V to III. The bandpass of the  $C_0(35 - 38)$  filter is analogous to the Strömgen  $u$  filter (VB68), which is known to be sensitive to the strength of the  $\lambda 3360$  NH band in globular cluster red giants (Grundahl et al. 2002).

The behaviour of  $C_0(35 - 38)$  versus  $[\text{Fe}/\text{H}]$  is shown in Figure 19. Two linear least-squares fits were calculated, one using the entire cluster data set (fit  $c$  in Table 1), and a second restricted to clusters with reddening  $E(B - V)_{\text{H99}} \leq 0.3$  (fit  $d$ ). Both fits are shown in Figure 19. Although  $C_0(35 - 38)$

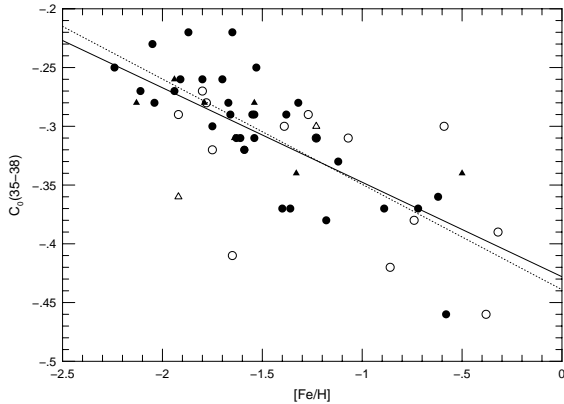


**Fig. 19.** The integrated  $C_0(35 - 38)$  colours of Milky Way globular clusters versus metallicity. Symbols are the same as for Figure 1. Two linear least-squares fits are shown. The solid line gives the fit to all clusters (fit  $c$  in Table 1), whereas the dashed line shows the fit obtained when considering only clusters with reddenings of  $E(B - V)_{H99} \leq 0.3$  (fit  $d$ ).

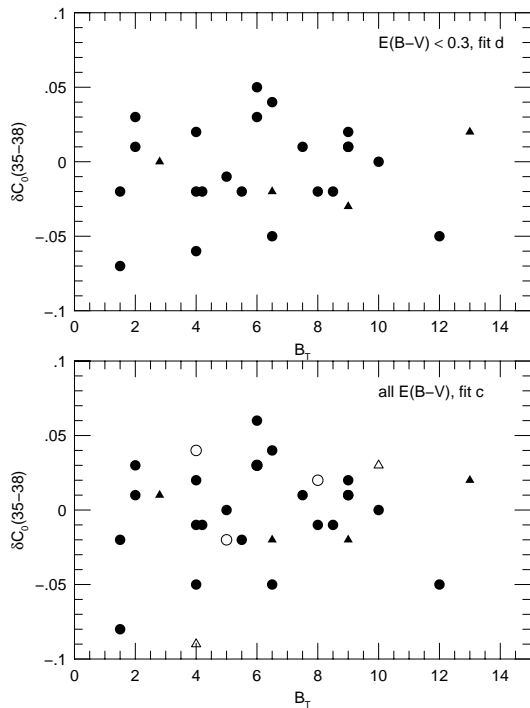


**Fig. 20.** The  $\delta C_0(35 - 38)$  residuals versus the horizontal branch parameter  $B_T$ . Residuals about two different least-squares fits are shown, one fit being derived from the full dataset of  $C(35 - 38)$  colours (fit  $c$ ), the other being based only on clusters with reddenings  $E(B - V)_{H99} \leq 0.3$  (fit  $d$ ).

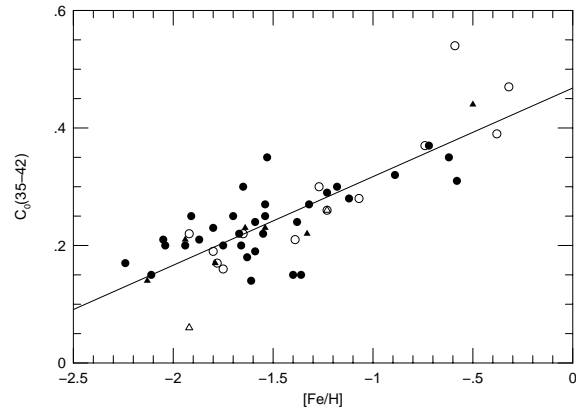


**Fig. 21.** The integrated  $C_0(35 - 42)$  colours of Milky Way globular clusters versus metallicity. Symbols are the same as for Figure 1. The linear least-squares fit (solid line) is based on all clusters for which data are available. The coefficients are listed as fit  $e$  in Table 1.

shows a correlation with  $[\text{Fe}/\text{H}]$  it is not as sensitive as the other DDO colours discussed above. Also in contrast to the previous colours,  $C_0(35 - 38)$  becomes more negative with increasing  $[\text{Fe}/\text{H}]$ , rather than more positive. With increasing metallicity the giant branch and main sequence turnoff becomes cooler, and the hydrogen lines from the cluster giants get weaker, thereby increasing the flux in the  $C35$  filter relative to the  $C38$  filter. As usual,  $\delta C_0(35 - 38)$  residuals were calculated about each fit and are plotted versus the horizontal branch parameter  $B_T$  in Figure 20. The notable result is that  $\delta C_0(35 - 38)$  does not correlate with  $B_T$  (see also Table 2).

The lack of a dependence on HB morphology in the  $C_0(35 - 38)$  colour appears to be due to the  $C35$  and  $C38$  passbands both being sensitive to blue HB stars. Figure 21 shows the rather non-standard colour  $C_0(35 - 42)$  versus  $[\text{Fe}/\text{H}]$ , together with a linear least-squares fit (labelled  $e$  in Table 1) based on all clusters with available data. There is a clear correlation with  $[\text{Fe}/\text{H}]$ , but it has a smaller slope than the  $C_0(38 - 42)$  colour-metallicity relation. The  $\delta C_0(35 - 42)$  residuals about fit  $e$  are plotted in Figure 22, where they show some trend with  $B_T$ , although on account of some outliers the resulting correlation coefficient of  $r = -0.29$  is modest. The  $\delta C_0(35 - 42)$  residuals at a given  $B_T$  tend to be comparable to those in the  $C_0(38 - 42)$  colour. Consequently, in forming the  $C_0(35 - 38)$  colour, the HB effects in the  $C35$  and  $C38$  bands tend to cancel out, with little consequent dependence upon  $B_T$  left.

This cancellation effect is promoted by the presence of Balmer line absorption in both the  $C35$  and  $C38$  bandpasses. Also reducing the sensitivity of  $C_0(35 - 38)$  to HB morphology could be the way in which Balmer line strengths vary with effective temperature along the horizontal branch. Figure 3 of McClure & van den Bergh (1968) shows how  $C_0(35 - 38)$  behaves as a function of spectral type between B0 and F0 for Population I dwarfs. This colour has a maximum value at A0, and is similar in value for F0 and mid-

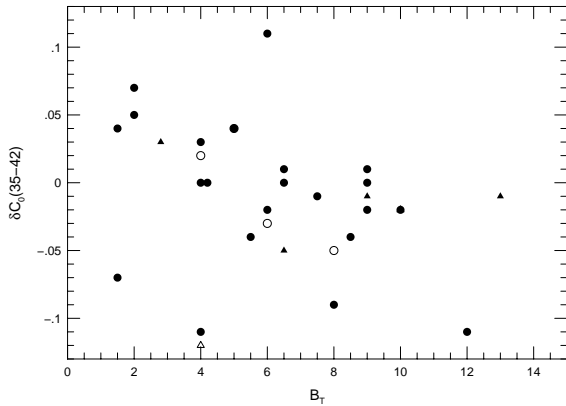


**Fig. 22.** The  $\delta C_0(35 - 42)$  residuals about fit  $e$  versus the horizontal branch parameter  $B_T$ . Symbols are the same as for Figure 1.

B spectral types. Thus, extending a horizontal branch hotter than an effective temperature of 10,000 K would not cause  $C_0(35 - 38)$  to become any redder, and may instead produce a degeneracy in colour as a function of  $B_T$ .

#### 4. Washington Photometry

The Washington system (Canterna 1976) has received substantial use in the study of extragalactic globular clusters (e.g., Geisler & Forte 1990; Harris et al. 1992; Lee & Geisler 1993; McLaughlin et al. 1995; Ostrov, Forte, & Geisler 1998; Forte et al. 2001; Harris, Harris, & Geisler 2004). This system originally had two metallicity indicators denoted  $M - T_1$  and  $C - M$ , the later of which is particularly useful for metal-poor stars (Geisler 1986; Geisler, Claria, & Minniti 1991). Extragalactic globular cluster studies have tended to employ the  $C - T_1$  colour as a metallicity index following the work of Geisler & Forte (1990). Since the bandpass of the  $C$  filter has an effective wavelength of 3910 Å and a FWHM of 1100 Å (Canterna 1976) it incorporates a number of Balmer lines. In principle therefore both the integrated  $C - M$  and  $C - T_1$  colours could be sensitive to the HB morphology of globular clusters. To investigate this possibility, we have used the integrated  $C - M$  and  $M - T_1$  colours of 51 GCs from Harris & Canterna (1977; H&C77), combined with the H99 reddenings and the metallicities described above. The H&C77 observations were obtained with telescopes at Manastash Ridge Observatory, Kitt Peak National Observatory, and Cerro Tololo Inter-American Observatory, equipped with pulse-counting photometers using RCA Ga-As photomultiplier tubes. Reddening ratios of  $E(M - T_1)/E(B - V) = 0.95$  and  $E(C - M)/E(B - V) = 1.14$  (Harris & Canterna 1977) were used to obtain the intrinsic colours  $(C - M)_0$ ,  $(M - T_1)_0$ , and  $(C - T_1)_0$ .

The  $(C - T_1)_0$  versus metallicity diagram and a linear fit to it are shown in Figure 23. The coefficients of this fit, which was made to the full sample, are given in row  $f$  of Table 1. The

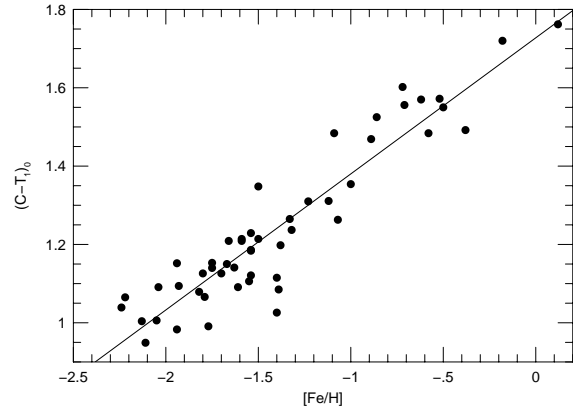


**Fig. 23.** The integrated  $(C - T_1)_0$  colours of Milky Way globular clusters versus  $[Fe/H]$  metallicity. A linear least-squares fit ( $f$  in Table 1) is shown.

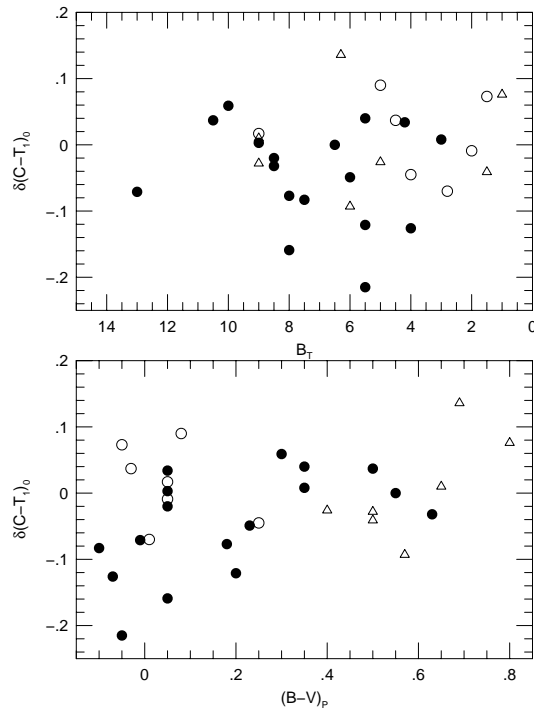


**Fig. 24.** Residuals  $\delta(C - T_1)_0$  relative to the least-squares fit  $f$  versus the horizontal branch parameters  $B_T$  and  $(B - V)_p$ . Symbols here differ from the conventions used in previous figures, and are based on metallicity:  $[Fe/H] < -1.8$  (open circles),  $-1.8 \leq [Fe/H] \leq -1.3$  (filled circles),  $[Fe/H] > -1.3$  (open triangles).



colour residuals about the fit are plotted versus both HB parameters  $B_T$  and  $(B - V)_p$  in Figure 24. There may be a weak relation with  $(B - V)_p$ , but not with the blue-tail parameter  $B_T$  (see Table 2). The value of the Pearson linear correlation coefficient between  $\delta(C - T_1)_0$  and  $(B - V)_p$  is 0.36 for those 31 clusters that have both integrated Washington photometry and measured HB parameters. The symbols in Figure 24 refer to cluster metallicity, with filled circles denoting the metallicity range  $-1.8 \leq [\text{Fe}/\text{H}] \leq -1.3$  wherein  $(B - V)_p$  shows the greatest scatter due to the second-parameter effect. The intermediate-metallicity clusters with HB modal colours of  $(B - V)_p < 0.0$  do have relatively blue  $(C - T_1)_0$  residuals, which may suggest that this Washington colour is sensitive to HB morphology if the blue side of the RR Lyrae gap is sufficiently populated. However, this tentative trend is heavily weighted by three clusters with  $[\text{Fe}/\text{H}] \approx -1.4$ , namely NGC 288, NGC 6218, and NGC 6402, for which  $\delta(C - T_1)_0$  is equal to  $-0.215$ ,  $-0.126$ , and  $-0.159$  respectively, the lowest values of any clusters in the sample. They fall farthest below the linear-fit line in Figure 23. If they are excluded from the sample the Pearson correlation coefficient drops to  $r = 0.20$ . Correlation coefficients for the  $\delta(C - T_1)_0$  residuals versus the GC structure properties  $\log \rho_0$ ,  $c$ , and  $b/a$  are listed in Table 2. In all three cases  $r < 0.1$ , with no evident correlations.

The  $(C - M)_0$  and  $(M - T_1)_0$  colours are plotted versus  $[\text{Fe}/\text{H}]$  in Figure 25. Linear fits to the full data sets are shown, the coefficients of which are listed in Table 1. The corresponding  $\delta(C - M)_0$  residuals are plotted versus  $B_T$  and  $(B - V)_p$  in Figure 26. The trends seen for  $\delta(C - M)_0$  are much the same as for  $\delta(C - T_1)_0$ , there being no significant correlation with  $B_T$  for the full sample of clusters, or with  $(B - V)_p$  for clusters having horizontal branches with  $(B - V)_p > 0$ . There may be a tendency for some intermediate-metallicity clusters with  $(B - V)_p < 0.1$  to have a blue  $(C - M)_0$  excess. However, as with the case with the  $(C - T_1)_0$  colour, this tendency is due largely to the three clusters NGC 288, NGC 6218, and NGC 6402. If these three clusters are excluded, the correlation coefficient drops from  $r = 0.36$  to 0.20.

The sensitivity of  $(M - T_1)_0$  to metallicity is much less than for either of the colours including the  $C$  band, as can be seen from Figure 6 of Harris et al. (1992). The  $\delta(M - T_1)_0$  residuals behave similarly to those of the other Washington colours discussed above. There is no obvious correlation with  $B_T$ , and while there may be a slight trend with  $(B - V)_p$ , it is again strongly influenced by the three clusters NGC 288, NGC 6218, and NGC 6402 (see Table 2). In summary, the behaviour of the Washington colours could be similar to that of  $B - V$ , in that they may be more sensitive to the modal colour of the horizontal branch than to the extent of the BHB tail.

## 5. Summary and Conclusions

In summary, we find that the integrated  $U - B$  colours of Milky Way globular clusters do exhibit a significant dependence on blue horizontal branch morphology as parameterised by the  $B_T$  index. The situation for the  $B - V$

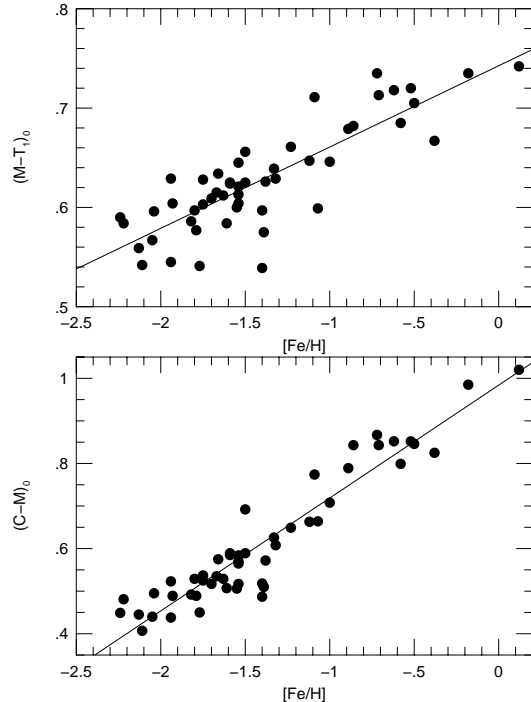


**Fig. 25.** The integrated Washington  $(C - M)_0$  and  $(M - T_1)_0$  colours of Milky Way globular clusters are plotted versus metallicity. Linear least-squares fits to each dataset are shown, with the coefficients listed as fits  $g$  and  $h$  respectively in Table 1.

colour is rather equivocal, with some very modest dependence possibly being discerned with respect to the HB parameter  $(B - V)_p$ , but not the blue-tail parameter  $B_T$ . However, this possible effect is rather sensitive to clusters of high reddening. Among intermediate-metallicity GCs, any significant second-parameter effect on integrated  $(B - V)_0$  seems to be limited to a small subset of objects whose HBs have relatively blue modal colours but not necessarily extended blue tails. The  $V - I$  colour evinces considerable scatter about a mean colour-metallicity relation for the Milky Way globulars, with the fit obtained being influenced by the extent to which the most heavily reddened clusters are included in the sample. The origin of the scatter in  $V - I$  at a given  $[\text{Fe}/\text{H}]$  is not clear. There may be a modest relation with the cluster concentration  $c$  in the sense expected if some high-concentration clusters are diminished in the number of red giants in their cores. However, any such intrinsic scatter is again at a level comparable to the observational uncertainties, and furthermore there is no evidence of a difference in mean  $UBVI$  colours between core-collapse and non-core-collapse clusters at a given metallicity. Evidence for any correlations between integrated colours and GC structure is weak at best.

Based on the values of  $\sigma_C/\beta$  from Table 1, and the degree of sensitivity (or otherwise) to horizontal branch morphology, we suggest that the  $B - V$  or  $B - I$  colours may be preferable

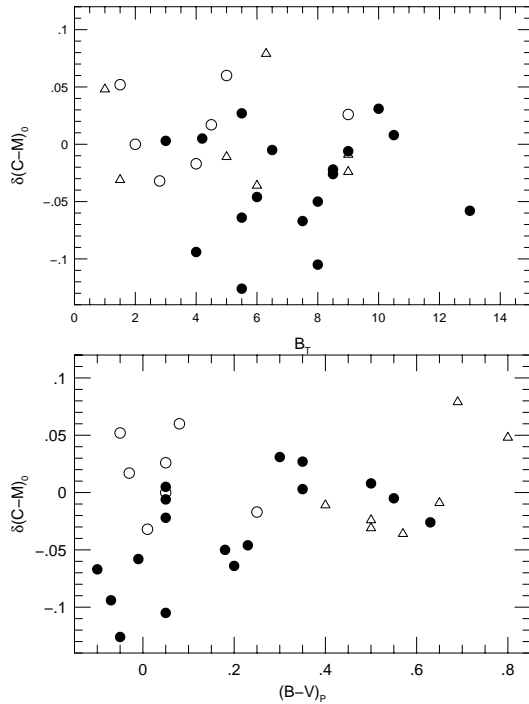


**Fig. 26.** The  $\delta(C - M)_0$  residuals about the linear fit  $g$  from Table 1 (also shown in Figure 25) versus the horizontal branch parameters  $B_T$  and  $(B - V)_p$ . Symbols here are based on metallicity and have the same designation as for Figure 24:  $[\text{Fe}/\text{H}] < -1.8$  (open circles),  $-1.8 \leq [\text{Fe}/\text{H}] \leq -1.3$  (filled circles),  $[\text{Fe}/\text{H}] > -1.3$  (open triangles).

metallicity indicators to the often-employed Cousins  $V - I$ . The latter colour has the appeal that globular clusters have higher integrated fluxes in the  $V$  and  $I$  passbands than in the  $B$  band. However, until the source of the relatively large scatter about the observed  $(V - I)_0$ -metallicity relation for Milky Way GCs can be pinned down, the application of this colour as a metallicity diagnostic warrants further investigation.

On the basis of Figure 7, a globular cluster having a horizontal branch with a very elongated blue tail (say  $B_T > 8$ ) could have a  $(U - B)_0$  colour that is  $\Delta(U - B) = 0.05 - 0.10$  mag bluer than another GC with the same  $[\text{Fe}/\text{H}]$  but a less extreme BHB (with  $B_T \sim 2$  to 4). If the  $(U - B)_0$  colour were being used as a metallicity diagnostic, then the  $[\text{Fe}/\text{H}]$  of the former cluster could be underestimated by  $\Delta[\text{Fe}/\text{H}] = \Delta(U - B)_0/\beta = 0.25$  to 0.5 dex, based on the slope of fit A from Table 1. This rather considerable effect illustrates the level to which the  $(U - B)_0$  colour could be compromised for metallicity estimation by horizontal-branch effects. In the case of the  $(B - V)_0$  colour, there may be a small number of clusters in Figures 9 and 10 which have  $\delta(B - V)_0 < -0.05$  due to a blue horizontal branch. An effect of this magnitude would cause the  $(B - V)_0$  colour to underestimate the metallicity of a globular cluster by  $> 0.4$  dex. Thus, although we find that any significant effect of HB morphology

on  $(B - V)_0$  colour may be limited to a small fraction of GCs in the Milky Way, if it does occur it can lead to quite substantial errors in the inferred metallicity.

The DDO  $C_0(38 - 42)$  colour is found to be sensitive to the blue tail of the horizontal branch, as parameterised through the index  $B_T$ , although no such effect is seen in the  $C_0(42 - 45)$  colour. Thus, as with the case for  $U - B$ , the HB blue tail seems to be most effective in modifying colours which have one bandpass blueward of  $4000 \text{ \AA}$ . By contrast, in the case of the  $C_0(35 - 38)$  colour, which has both bandpasses blueward of  $4000 \text{ \AA}$ , the effects of hydrogen line absorption in each band partially cancel out, so that it exhibits less variation with  $B_T$  than do either  $C_0(38 - 42)$  or  $C_0(35 - 42)$ . In the case of the integrated  $C_0(38 - 42)$  colour, extremes of BHB morphology might cause an effect of  $\sim 0.05$  mag, based on the lower panel of Figure 18. This could lead to an error in  $[\text{Fe}/\text{H}]$  of  $\sim 0.2$ - $0.25$  dex if the colour was being used as a metallicity diagnostic.

The Washington colours may be modestly affected by a second parameter, with there being more evidence for a correlation between colour residuals and  $(B - V)_p$  than with  $B_T$ , although this conclusion is greatly dependent on the data for three clusters with  $[\text{Fe}/\text{H}] \approx -1.4$ . As such, the Washington colours may behave with respect to HB morphology in a manner that is more similar to that of the integrated  $B - V$  colour than  $U - B$ . Nonetheless, perhaps the most valid conclusion is that any influence of the second parameter on integrated Washington colours is near the limit of the uncertainties in the available measurements.

The implication for the study of extragalactic globular clusters is that in the Milky Way GC system, none of the commonly used colours  $B - V$ ,  $V - I$ ,  $B - I$ , or  $C - T_1$ , show deviations from colour-metallicity relations that can be systematically related to horizontal branch morphology. Most of the residuals that we find in these colours may be more attributable to errors in observational measurement or interstellar reddening. A similar conclusion may be applicable to the Sloan colour  $g - z$  (which has seen increasing use in the study of extragalactic globular clusters), since the bandpasses are similar to  $B - I$ . There may be weak horizontal branch effects in  $B - V$  and  $C - T_1$ , but these are at the limit of the observational uncertainties. This conclusion is not without caveats, however, due to (i) the restricted metallicity range of Milky Way globular clusters compared to some GC systems in external galaxies, and (ii) the ever-lurking second-parameter effect, which may behave differently in external systems.

*Acknowledgements.* We are grateful to Daniel Harbeck for valuable discussions during the formative stages of this work.

## References

- Aaronson, M., Cohen, J. G., Mould, J., Malkan, M.: 1978, ApJ 223, 824  
 Armandroff, T. E., & Da Costa, G. S.: 1991, AJ 101, 1329  
 Barmby, P., Huchra, J. P.: 2000, ApJ 531, L29  
 Barmby, P., Huchra, J. P., Brodie, J. P., Forbes, D. A., Schroder, L. L., Grillmair, C. J.: 2000, AJ 119, 727  
 Bedin, L. R., Piotto, G., Zoccali, M., Stetson, P. B., Saviane, I., Casisi, S., Bono, G.: 2000, A&A 363, 159

- Bell, R. A., Dickens, R. J., Gustafsson, B.: 1979, *ApJ* 229, 604
- Bica, E. L. D., Pastoriza, M. G.: 1983, *Ap&SS* 91, 99
- Brocato, E., Castellani, V., Poli, F. M., Raimondo, G.: 2000, *A&A* 146, 91
- Brodie, J. P., Huchra, J. P.: 1990, *ApJ* 362, 503
- Buonanno, R., Caloi, V., Castellani, V., Corsi, C., Fusi Pecci, F., Gratton, R.: 1986, *A&AS* 66, 79
- Buonanno, R., Fusi Pecci, F., Cappellaro, E., Ortolani, S., Richtler, T., Geyer, E. H.: 1991, *AJ* 102, 1005
- Canterna, R.: 1976, *AJ* 81, 228
- Catelan, M., Borissova, J., Sweigart, A. V., Spassova, N.: 1998, *ApJ*, 494, 265
- Catelan, M., de Freitas Pacheco, J. A.: 1995, *A&A* 297, 345
- Claria, J. J., Minniti, D., Piatti, A. E., Lapasset, E.: 1994a, *MNRAS* 268, 733
- Claria, J. J., Piatti, A. E., Lapasset, E.: 1994b, *PASP* 106, 436
- Cohen, J. G., Matthews, K.: 1994, *AJ* 108, 128
- Covino, S., Pasinetti, L. E., Malagnini, M. L., Buzzoni, A.: 1994, *A&A* 289, 775
- De Angeli, F., Piotto, G., Cassisi, S., Busso, G., Recio-Blanco, A., Salaris, M., Aparicio, A., Rosenberg, A.: 2005, *AJ* 130, 116
- de Freitas Pacheco, J. A., Barbuy, B.: 1995, *A&A* 302, 718
- Djorgovski, S., Piotto, G.: 1992, *AJ* 104, 2112
- Djorgovski, S., Piotto, G., Phinney, E. S., Chernoff, D. F.: 1991, *ApJ* 372, L41
- Forte, J. C., Geisler, D., Ostrov, P. G., Piatti, A. E., Gieren, W.: 2001, *AJ* 121, 1992
- Frogel, J. A., Persson, S. E., Cohen, J. G.: 1980, *ApJ* 240, 785
- Fusi Pecci, F., Ferraro, F. R., Ballazini, M., Djorgovski, S., Piotto, G., Buonanno, R.: 1993, *AJ* 105, 1145
- Geisler, D.: 1986, *PASP* 98, 762
- Geisler, D., Claria, J. J., Minniti, D.: 1991, *AJ* 102, 1836
- Geisler, D., Forte, J. C.: 1990, *ApJ* 350, L5
- Grundahl, F., Briley, M., Nissen, P. E., Feltzing, S.: 2002, *A&A* 385, L14
- Hamuy, M.: 1984, *A&AS* 57, 91
- Hanes, D. A., Brodie, J. P.: 1985, *MNRAS* 214, 491
- Harris, G. L. H., Geisler, D., Harris, H. C., Hesser, J. E.: 1992, *AJ* 104, 613
- Harris, G. L. H., Harris, W. E., Geisler, D.: 2004, *AJ* 128, 723
- Harris, H. C., Canterna, R.: 1977, *AJ* 82, 798
- Harris, W. E.: 1974, *ApJ* 192, L161
- Harris, W. E.: 1996, *AJ* 112, 1487
- Harris, W. E., Racine, R.: 1979, *ARA&A* 17, 241
- Howell, J. H., Guhathakurta, P., Tan, A.: 2000, *AJ* 119, 1259
- Janes, K. A.: 1975, *ApJS* 29, 161
- Johnson, J. A., Bolte, M.: 1998, *AJ* 115, 693
- Kurth, O. M., Fritze-von Alvensleben, U., Fricke, K. J.: 1999, *A&AS* 138, 19
- Lee, H.-C., Yoon, S.-J., Lee, Y.-W.: 2000, *AJ* 120, 998
- Lee, M. G., Geisler, D.: 1993, *AJ* 106, 493
- Leitherer, C., et al.: 1996, *PASP* 108, 996
- Maraston, C.: 1998, *MNRAS* 300, 872
- Maraston, C., Thomas, D.: 2000, *ApJ* 541, 126
- Maraston, C.: 2005, *MNRAS* 362, 799
- McClure, R. D.: 1973, in: C. Fehrenbach, B. E. Westerlund (eds.), *Spectral Classification and Multicolor Photometry, IAU Symposium No. 50*, Riedel, Dordrecht, p. 162
- McLaughlin, D. E., Secker, J., Harris, W. E., Geisler, D.: 1995, *AJ* 109, 1033
- Moehler, S., Sweigart, A. V., Catelan, M.: 1999, *A&A* 351, 519
- Momany, Y., Piotto, G., Recio-Blanco, A., Bedin, L. R., Cassis, S., Bono, G.: 2002, *ApJ* 576, L65
- Newell, B., Sadler, E. M.: 1978, *ApJ* 221, 825
- Osborn, W.: 1973, *ApJ* 186, 725
- Ostrov, P. G., Forte, J. C., Geisler, D.: 1998, *AJ* 116, 2854
- Peterson, R. C., Carney, B. W., Dorman, B., Green, E. M., Landsman, W., Liebert, J., O'Connell, R. W., Rood, R. T.: 2003, *ApJ* 588, 299
- Philip, A. G. D., Cullen, M. F., White, R. E.: 1976, *UBV Color-Magnitude Diagrams of Galactic Globular Clusters, Dudley Observatory Report No. 11*, Dudley Observatory Press, Albany
- Press, W. H., Teukovsky, S. A., Vetterling, W. T., Flannery, B. P.: 1999, *Numerical Recipes in Fortran 77, 2nd ed.*, Cambridge University Press, Cambridge
- Puzia, T. H., et al.: 2005, *A&A* 439, 997
- Racine, R.: 1973, *AJ* 78, 180
- Reed, B. C.: 1985, *PASP* 97, 120
- Reed, B. C., Hesser, J. E., Shawl, S. J.: 1988, *PASP* 100, 545
- Rey, S.-C., Yoon, S.-J., Lee, Y.-W., Chaboyer, B., Sarajedini, A.: 2001, *AJ* 122, 3219
- Rich, R. M., Sosin, C., Djorgovski, S. G., Piotto, G., King, I. R., Renzini, A., Phinney, E. S., Dorman, B., Liebert, J., Meylan, G.: 1997, *ApJ* 484, L25
- Rosenberg, A., Saviane, I., Piotto, G., Aparicio, A.: 1999, *AJ* 118, 2306
- Rutledge, G. A., Hesser, J. E., Stetson, P. B., Mateo, M., Simard, L., Bolte, M., Friel, E. D., Copin, Y.: 1997a, *PASP* 109, 883
- Rutledge, G. A., Hesser, J. E., Stetson, P. B.: 1997b, *PASP* 109, 907
- Sandage, A., Wildey, R.: 1967, *ApJ* 150, 469
- Schiavon, R. P., Rose, J. A., Courteau, S., MacArthur, L. A.: 2004, *ApJ* 608, L33
- Sil'chenko, O. K.: 1983, *SvAL* 9, 145
- Spearman, C.: 1904, *Am. J. Psychol.* 15, 72
- Sung, H., Lee, S.-W.: 1987, *JKAS* 20, 63
- Tripicco, M. J., Bell, R. A.: 1991, *AJ* 102, 744
- van den Bergh, S.: 1967, *AJ* 72, 70
- Walker, A. R.: 1999, *AJ* 118, 432
- White, R. E., Shawl, S. J.: 1987, *ApJ* 317, 246
- Worthy, G.: 1994, *ApJS* 95, 107
- Yi, S.: 2003, *ApJ* 528, 202
- Zinn, R., West, M.: 1984, *ApJS* 55, 45